JOURNAL OF FOOD PROCESS ENGINEERING

JOURNAL OF FOOD PROCESS ENGINEERING

JOURNAL OF FOOD PROCESS ENGINEERING

Journal of
FOOD PROCESS ENGINEERING

Coeditors: D.R. HELDMAN
R.P. SINGH

CONTENTS

MEASURING THE MECHANICAL PROPERTIES
OF APPLE TISSUE USING MODAL ANALYSIS

G. VAN WOENSEL, E. VERDONCK AND J. DE BAERDEMAEKER

[1]*Katholieke Universiteit te Leuven*
Laboratorium voor Landbouwwerktuigkunde
Kardinaal Mercierlaan 92
3030 Leuven (Heverlee), Belgium

ABSTRACT

Along with the grade of intactness, fruit firmness is an important factor for the quality criteria on which the consumers acceptance for apples is based.

Two methods for measuring the fruit firmness (a destructive one and a nondestructive one) are compared. The nondestructive method uses modal analysis to define the lower vibration modes. This enables the use of the 3-media elastic sphere model developed by Cooke and Rand (1973) to calculate the dynamic elastic moduli of the whole apples. The destructive method determines the dynamic elastic moduli of cylindrical samples of apple tissue. This method is based on the vibration characteristics of a mass-spring-damper system. This system consists of a cylindrical apple sample and a mass. Measuring the direct transfer function of this one-degree-of-freedom system results in values of its system parameters, from which the dynamic elastic moduli of the specimen can be calculated.

The results of the two methods applied on Golden Delicious apples were compared, and the suitability of each model was evaluated.

INTRODUCTION

The evaluation of fruit quality and eating maturity of apples requires the determination of those properties that affect the quality criteria on which the consumers acceptance is based. Fruit texture is, among others, an important parameter and efforts have been made for its measurement both in destructive and nondestructive dynamic tests.

From uniaxial compression tests the normal stress to failure was found to give useful information about the internal quality of the apples around the time they loose their acceptability for the consumer (Diehl and Hammann 1979; Tijskens 1979). Hence, static tests alone are not satisfactory in the quality evaluation of hard fruits.

Fruit can also be subjected to several dynamic tests to get information about its mechanical characteristics.

The frequency response of the fruit (acceleration divided by applied force) in the audio-frequency range has been investigated by several authors as a means for the nondestructive testing of fruit firmness. Abbott *et al.* (1968) suspended apples by their stem, applied a periodic mechanical excitation on the equator of the apple and measured the response on the top of the fruit.

Finney (1970) placed the fruit, with the stem-calix axis horizontal, on a force transducer which was mounted on a vibration exciter. The response was measured with an accelerometer on top of the fruit (i.e., 180° apart). These authors used the stiffness coefficient f^2m, with f the second resonant frequency of the apple and m the apple mass, as being a good texture parameter.

Cooke and Rand (1973) developed a conceptual framework for the interpretation and nondestructive resonance studies of the texture of intact fruits. They studied the resonant behaviour of intact fruits (e.g., apples), modelled as having three mechanical distinct, concentric, spherical regions. They arrived at a procedure by which the resonant frequency method can be used to find the elastic moduli for the flesh of intact fruits and vegetables which have approximately spherical geometry. From their calculations they concluded for freely vibrated fruit that the lowest resonant frequency corresponds to the first spheroidal vibration mode and that the second resonant frequency corresponds to a torsional mode. Cook (1972) calculated that the fresh shear modulus, noted in this mode as G_c is given by:

$$G_c = f^2 m^{2/3} \rho^{1/3}$$

with f the resonant frequency at the first spheroidal vibration mode,
m the apple mass,
ρ the apple flesh density (0.84 g cm^{-3} for Golden Delicious apples, Mohsenin (1970),
and CR a dimensionless conversion ratio.

The conversion ratio CR is dependent on the radii, mass density and shear moduli ratios of the apple skin, the apple flesh and the core.

In a theoretical study Cooke estimated CR as being in the range of 2.0 to 3.5. Based on Finney's data (1970), CR was estimated to be between 1.0 and 1.5.

The stiffness factor $S = f^2 m^{2/3}$ does not contain a mass dependence.

From Cooke's shear modulus, G_c, Young's modulus, E_c, can be calculated as

$$E_c = G_c \, 2 \, (1 + \nu)$$

or

$$E_c = S \, \rho^{1/3} \, CR \, 2 \, (1 + \nu)$$

with ν the Poisson ratio (for Golden Delicious apples this can be estimated as 0.25 (Mohsenin 1970).

The loss moduli associated with G_c and E_c can be calculated as

$$G'_c = 2 G_c \zeta_c$$

and

$$E'_c = 2 E_c \zeta_c$$

with ξ_c the damping ratio associated with the second resonant frequency.

Yong and Bilanski (1979) concluded from their experiments that the second resonant frequency in the Finney experiments corresponds with the spherical mode of vibration of the apple. Tangential accelerations to detect the torsional modes were not measured.

In studying the apple textural changes during storage Van Woensel and De Baerdemaeker (1983) used an experimental method similar to that of Finney. They found that the stiffness factor $f^2 m^{2/3}$, as defined by Cooke and Rand (1973), shows a sharp decline at the storage time when the fruit reaches its maturity climacterium, thereby confirming the usefulness of this method for detecting fruit firmness changes.

Resonant frequencies of cylindrical specimen can be used to calculate the moduli of elasticity and associated loss moduli, which are a measure of internal damping.

Dynamic mechanical properties can also be measured on samples of the apple tissue. Petrell et al. (1980) measured compressive complex moduli by subjecting tissue samples to sinusoidal compressive stresses, superimposed to a static load. They found that the complex modulus was influenced by changes in the cellular structure of the fruit.

Dynamic measurements can be simplified by considering a tissue sample loaded with a mass as a one degree of freedom vibration system. The stiffness and damping of such a system can be determined from its frequency response.

The objective of the work reported here is to obtain more information on the mode shapes associated with the second resonant frequencies that are used for the observations of fruit firmness changes.

Because of the ease of radial measurements in these firmness studies, the modal analysis was also limited to radial displacements. To confirm that the second resonant frequency is indeed associated with the first spheroidal vibration mode, as claimed by Yong and Bilanski, two different set-ups were used. In a second step it was attempted to compare the mechanical properties obtained from the nondestructive tests with those from dynamic measurements on fruit tissue samples using the derivations by Cooke.

MODAL ANALYSIS OF AN APPLE

Although an apple may look like a simple structure in making mechanical measurements a lot of problems are due to the high degree of weakness and the low mass density of the apple. For making the frequency response measurements required for modal analysis two different ways of fixing the fruit and applying the load were evaluated.

In set-up I, the apple was mounted on an electromagnetic exciter. A low-weight accelerometer (2.4 g) was glued on the apple skin. In set-up II, the apple was suspended on a thin elastic string, and excited by a hammer. The accelerometer was glued to the apple skin as in set-up I.

The electromagnetic exciter gives a force input which is fairly uniform over the frequency range from 0 to 1600 Hz, except at low frequencies (from 0 to 200 Hz) where a much higher force input was found. At the frequency of about 330 Hz a dip in the force spectrum could be observed (Fig. 1).

When hammer excitation was applied, a high excitation force was found in the frequency range from 0 to 500 Hz. But a weak force input was found for frequencies higher than 500 Hz. However, a good response was found over the frequency range from 0 to 1600 Hz (Fig. 2).

The dynamic behavior of the apple is affected by the fixation of the accelerometer and the connection to the electromagnetic exciter. In both set-ups and location of the accelerometer was fixed during the modal analysis test, while the force input location was changed. Thus, the influence of the accelerometer on the dynamic behavior of the apple was constant, and independent of the measurement location. In case of set-up I there is a perceptible change of the dynamic behaviour of the apple due to the connection apple-electromagnetic exciter. Comparing the acceleration transfer functions obtained by both set-ups, there is one additional resonant frequency (first resonant frequency) in the case where set-up I has been used.

It can be seen from Table 1 that in set-up I (where the electromagnetic exciter has been used) higher values for the damping (damping ratio, ξ, the ratio of the energy dissipated by the measuring sample to the elastic energy of the sample) and the resonant frequency are found.

To obtain the model parameters (frequencies, damping, residues) from the measured acceleration transfer functions, in case of set-up I, a nonstandard nonlinear curve-fitting procedure has been used. Due to the fact that the resonant frequencies depend on the measurement location, these values had to be calculated for each measurement. The residues were determined on the resonant frequencies and damping values, for each particular measurement location. For set-up II a standard nonlinear curve-fiting procedure could be used.

The mode shapes are shown in Fig. 3. Mode 1 is found only when set-up is used. This mode is a so-called rigid-body mode of the structure (apple). Here, the
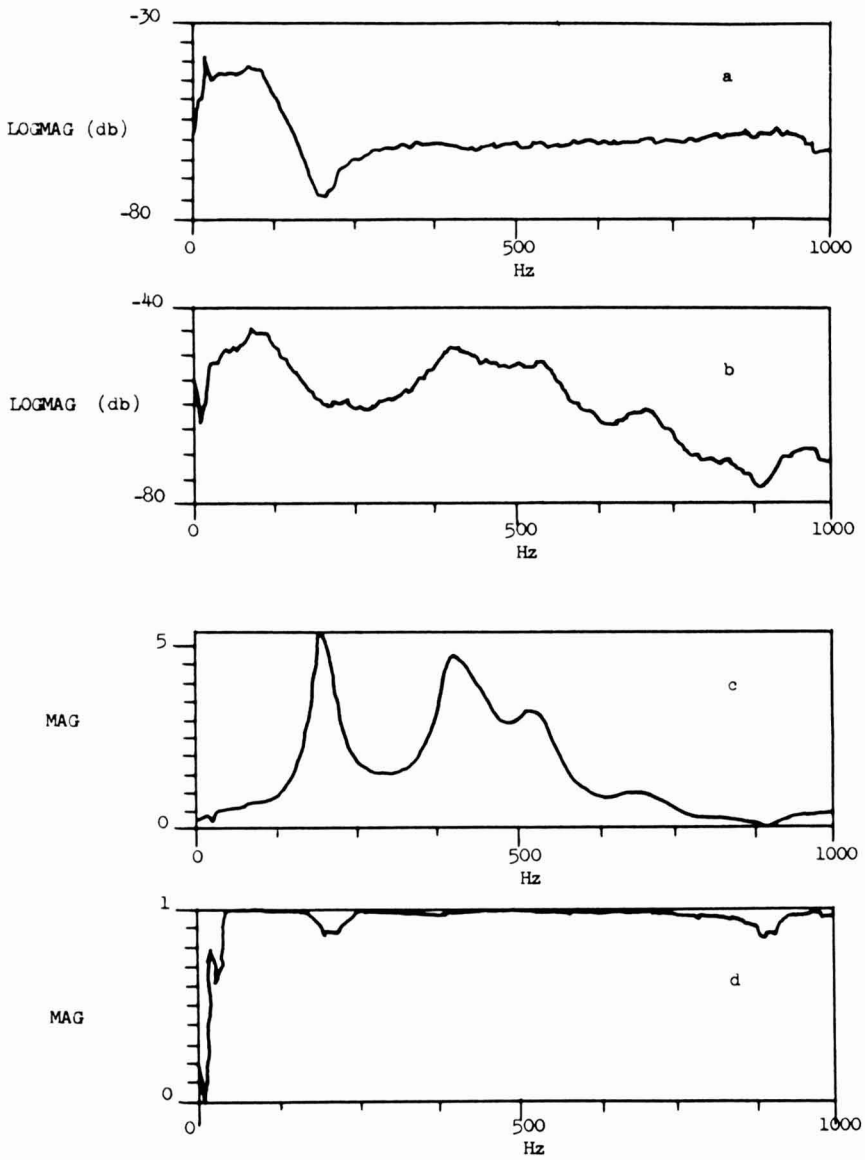
FIG. 1. TRANSFER FUNCTION MEASUREMENT USING SET-UP I

a. power function force-signal
b. power function acceleration-signal
c. transfer function
d. coherence function
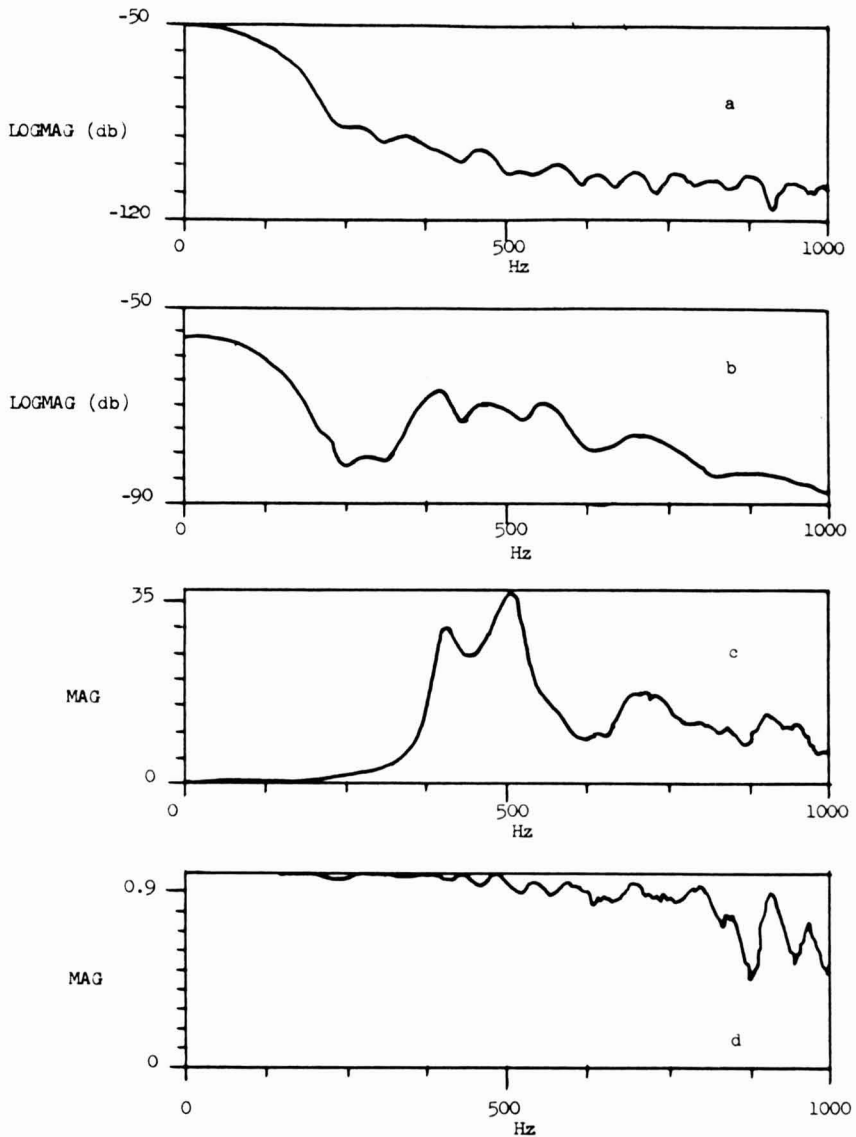
FIG. 2. TRANSFER FUNCTION MEASUREMENT USING SET-UP II

a. power function force-signal
b. power function acceleration-signal
c. transfer function
d. coherence function

TABLE 1.
COMPARISON OF THE FREQUENCY AND DAMPING VALUES
OBTAINED BY BOTH SET-UPS

Set-up mode	Frequency (Hz)		Damping ratio (%)	
	I	II	I	II
1	329.2	–	7.5	–
2	662.9	641.8	4.2	4.0
3	879.6	829.9	5.5	5.2

apple is not deformed, except near the support location where deformations oc-
cur due to the excitation force on the weak apple tissue. Mode 2 and 3 are the
spherical modes which are important for our study. Normally two modes are
found instead of one (referring to Cooke's spheroidal modal). This is due to the
fact that the apple is not a perfect sphere. The (theoretically) unique spheroidal
mode splits in two modes, corresponding to two principal axes of the apple
cross-section. The more the apple differs from a sphere, the larger the difference
between the resonant frequencies of mode 2 and 3.
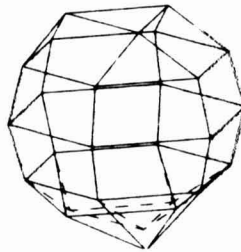
Mode 1: 329 Hz, front view
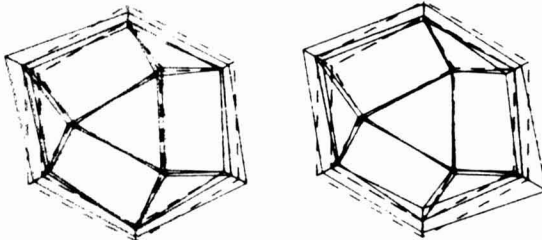
Mode 2: 663 Hz, top view   Mode 3: 880 Hz, top view.

FIG. 3. MODE SHAPES OBTAINED BY M.A. USING SET-UP I

It follows that care should be taken in interpreting the results obtained from modal analysis tests, depending on the measuring set-up used. The connection apple-exciter has a stiffening and a damping effect on the dynamic behavior of the apple. A rise of the resonant frequencies of 5% was found. The connection apple-exciter also causes one additional rigid-body mode, which has a resonant frequency of 329 Hz.

DIRECT MEASUREMENT OF YOUNG's MODULUS

For a direct measurement of the elastic modulus of the apple flesh, a measurement set-up is used, which is quite similar to the one used for the nondestructive tests.

A cylindrical sample of apple tissue, with mass M_s, loaded with a mass M is placed on a force transducer, mounted on a vibrating exciter. The exciter is driven by a pseudo-random noise signal with a bandwidth of 400 Hz.

Again a low mass accelerometer is placed on the top of the system in the same direction as the load cell (Fig. 4). This system corresponds to a mass-spring-damper system as shown in Fig. 5. This is a configuration of a mass m, a spring with spring constant k, and a damper with damping constant c. The mass m is equal to M if the sample mass can be ignored.
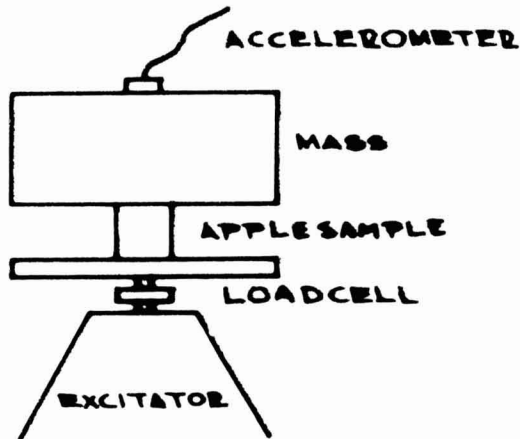
FIG. 4. MEASUREMENT SET-UP FOR THE DESTRUCTIVE DYNAMIC TEST
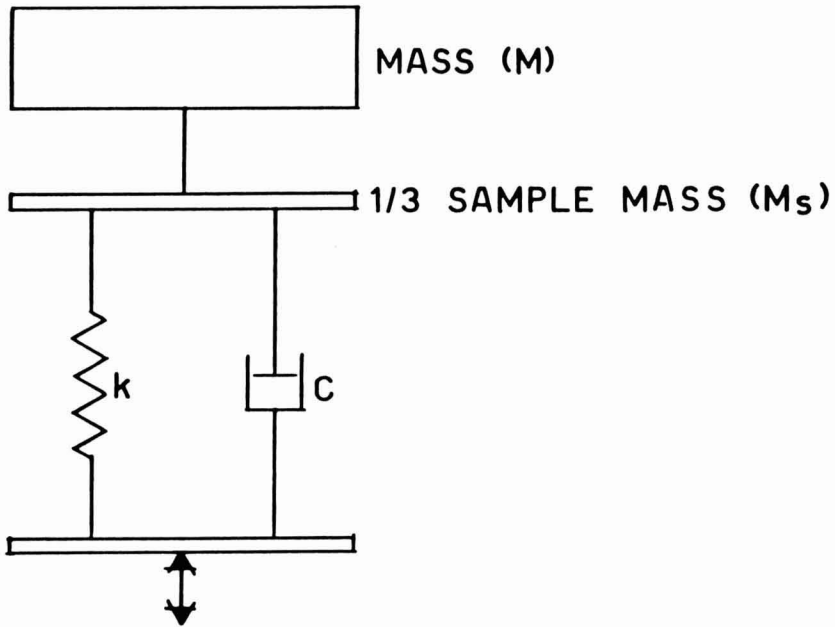
FIG. 5. MASS-SPRING-DAMPER SYSTEM CORRESPONDING TO
THE EXPERIMENTAL SYSTEM SHOWN IN FIG. 4

When a force f(t) is working on this system, the dynamic equilibrium is
described by the following differential equation:

$$m \ddot{x} + c \dot{x} + k x = f(t)$$

Fourier transforming and manipulating this equation results in the acceleration
transfer function:

$$\frac{\ddot{X}(\omega)}{F(\omega)} = \frac{- \omega^2 / k}{1 - \omega^2 / \omega_n^2 + 2j (\omega / \omega_n) \xi}$$

The ratio of the Fourier Transform of the accelerometer signal to that of the
force signal is calculated by a structural dynamics analyzer. An acceleration
transfer function is obtained as shown in Fig. 6. This transfer function results in
a value for the resonant frequency f_n of the vibrating system and an associated
damping ratio ξ.
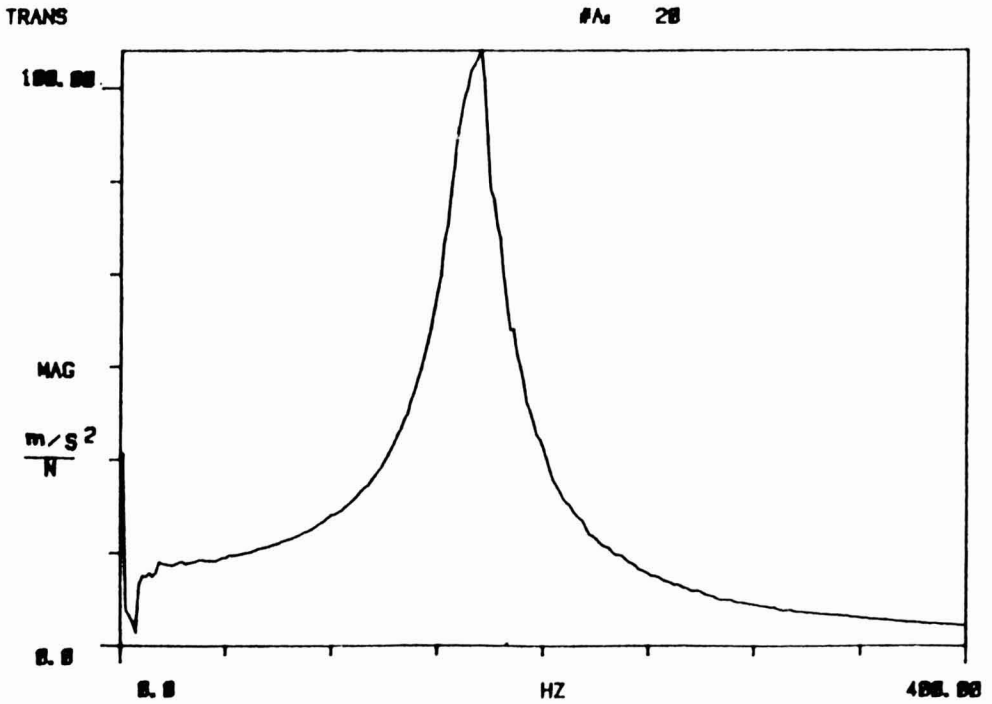
FIG. 6. DIRECT TRANSFER FUNCTION OF A VIBRATING CYLINDRICAL
APPLE SAMPLE LOADED WITH A MASS

From f_n and ξ, the spring stiffness k and the damping constant c can be calculated and finally, Young's modulus E and corresponding loss modulus E' of the measured sample are found by the equations:

$$E = k \; 1 \; / \; A \quad = \omega_n^2 . m . \quad 1/A$$

and

$$E' = c \; \omega_n (1 \; / \; A) \quad = \omega_n . (L/A) . \; \xi \; .2. \sqrt{km}$$

where 1 is the sample length and A is the cross section area of the apple specimen and $\omega_n = 2\Pi \frac{f}{\eta}$.

COMPARISON OF THE RESULTS
OBTAINED BY BOTH METHODS

The apples tested were forty Golden Delicious apples over a wide range of maturity stages. Each apple was subjected first to a nondestructive resonance test. Thereafter cylindrical samples were cut from the apple to be subjected to a vibration test.

Young's modulus E versus stiffness coefficient S is shown in Fig. 7. There exists a linear relationship between E and S with correlation factor r = 0.981. From this relationship the value of the dimensionless conversion ratio CR can be estimated using formula 1. Approximating ρ as 0.84 and ν as 0.25 (Mohsenin 1970); the value of CR is 2.2. This value does agree well with the range for CR between 2.0 and 3.5 derived by Cooke (1972).
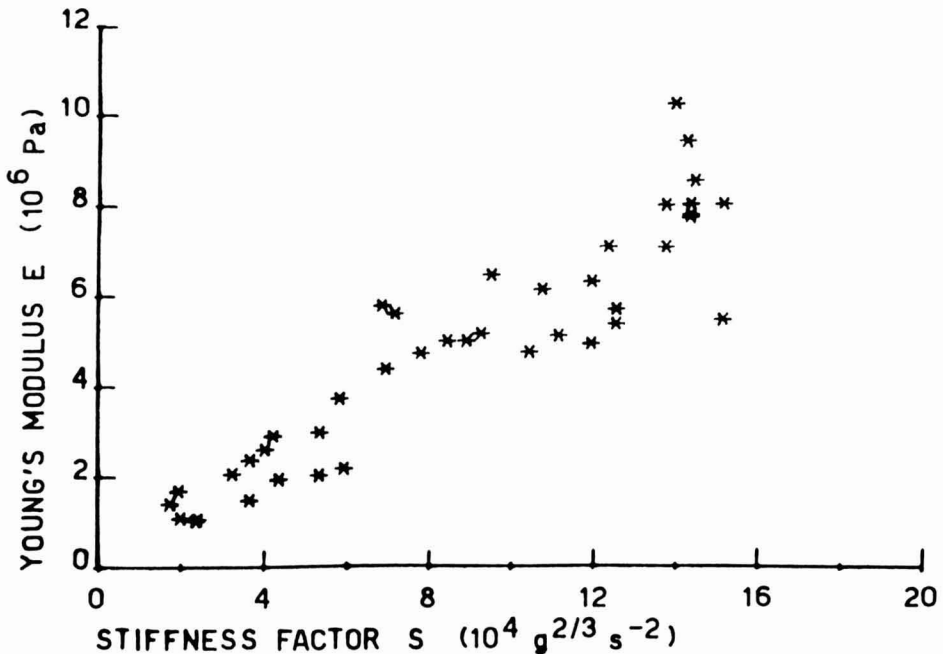
FIG. 7. RELATION BETWEEN THE YOUNG MODULUS E, OBTAINED IN A
DESTRUCTIVE DYNAMIC TEST, AND THE STIFFNESS FACTOR S,
DERIVED FROM THE VIBRATION OF A WHOLE APPLE

The damping ratio ξ derived in the nondestructive test seems to correlate highly with properties as the Young modulus and the corresponding loss modulus E and E', measured in the destructive way, and with the second resonant frequency f and the stiffness coefficient S.

The damping ratio derived from the vibration tests on cylindrical samples does not correlate with any other measured system parameter. Probably this damping ratio is strongly influenced by the presence of a thin water film between the apple sample and the loading mass or the vibrating plate. A more detailed discussion of the measurement results is given in (Van Woensel *et al.* 1987).

CONCLUSIONS

In this study dynamic tests were evaluated for their suitability in obtaining parameters related to fruit texture. Using modal analysis of a vibrating fruit it was shown that the commonly used second resonant frequency in nondestructive texture measurements corresponds to a spherical mode shape. A similar mode shape is found at different frequencies due to the nonspherical apple shape. The first vibration mode in tests with apples placed on a vibration exciter corresponds to a rigid-body mode of the fruit, i.e., a displacement of the center of the fruit. Since this resonant frequency depends on local skin and flesh properties, this mode is indeed unreliable as a measure of fruit firmness. The question as to whether a spheroidal mode or a torsional mode has the lowest resonant frequency remains unsolved as no tangential measurements have been done.

Based on the nondestructive dynamic measurements, especially of the resonant frequencies, the elastic properties of the fruit flesh can be derived. A method was described for direct measurements of these properties, and it was found that the values obtained with both methods were in good agreement.

ACKNOWLEDGMENT

REFERENCES

ABBOTT, J.A., BACHMAN, G.S., CHILDERS, R.F., FITZGERALD, J.V. and MATUZIK, F.J. 1968. Sonic techniques for measuring texture of fruits and vegetables. Food Technol. *22*, (635), 101–112.

COOKE, J.R. 1972. An interpretation of resonant behaviour of intact fruits and vegetables. Trans. of the ASAE, *15*(6), 1075.

COOKE, J.R. and RAND, R.H. 1973. A mathematical study of resonance in intact fruits and vegetables using a 3-media elastic sphere model. J. Agric. Engng. Res., *18*, 141–157.

DIEHL, K.C. and HAMANN, D.D. 1979. Structural failure in selected fruits and vegetables. J. Texture Studies, *10*, 371–400.

FINNEY ESSEX, JR., E. 1970. Mechanical resonance within Red Delicious apples and its relation to fruit texture. Trans. of the ASAE, *13*(2), 177–180.

MOHSENIN, N.N. 1970. *Physical properties of plant and animal materials.* Gordon & Breach Science Publishers, London.

PETRELL, R.J., MOHSENIN, N.N. and WALLNER, S. 1980. Dynamic mechanical properties of apple cortex in relation to sample location and ripening. J. Texture Studies, *12*, 217–229.

TIJSKENS, I.M.M. 1979. Texture of Golden Delicious apples during storage. Lebensm.-Wiss.u.-Technol. *12*, 138–142.

VAN WOENSEL, G. and DE BAERDEMAEKER, J. 1983. Mechanical properties of apples during storage. Lebensm.-Wiss.u.-Technol., *16*(6) 367–371.

VAN WOENSEL, G., WOUTERS, A. and DE BAERDEMAEKER, J. 1987. Relation between mechanical properties of Apple fruit and sensory quality. J. Food Proc. Eng. *9*, 173–189.

YONG, Y.C. and BILANSKI, W.K. 1979. Modes of vibration of spheroids at the first and second resonant frequencies. Trans. of the ASAE, *22*(6), 1463–1466.

MATHEMATICAL MODELLING OF RADIAL CONTINUOUS CROSSFLOW AGRICULTURAL DRYERS

STEFAN CENKOWSKI

The Department of Agricultural Engineering
University of Manitoba
Winnipeg, Manitoba, R3T 2N2, Canada

and

SHAHAB SOKHANSANJ

The Department of Agricultural Engineering
University of Saskatchewan
Saskatoon, Saskatchewan, S7N 0W0, Canada

ABSTRACT

Circular grain dryers in which grainflow is continuous and airflow is in radial direction are widely used as on-farm grain dryers. A concurrentflow drying model is adapted to the crossflow drying of the moving bed of grain. The simulated air and grain temperatures and moisture contents of wheat and corn samples were compared to the experimental drying of these grains in laboratory dryers. The results show that the model can be used to describe temperature of grain within 1 °C and moisture content within 0.3 % w.b.

INTRODUCTION

Circular grain dryers of the type shown in Fig. 1 are commonly used for on-farm drying of agricultural grains. The dryer consists of two concentric vertical cylinders made of perforated sheet metal. Grain moves down between the two cylinders while the hot air flows from the inner chamber to the outside, in a right angle to the direction of grain flow. Partially dried grain is lifted to the top of the drying chamber by a vertical auger for recirculation. Grain recirculates and drying continues until a final moisture content is achieved. The grain is then cooled in the drier by turning off the burner and forcing unheated air through the grain.

Thompson *et al.* (1968), Bakker-Arkema *et al.* (1974), O'Callahan *et al.* (1971), and Bruce (1984) developed mathematical models of grain drying.
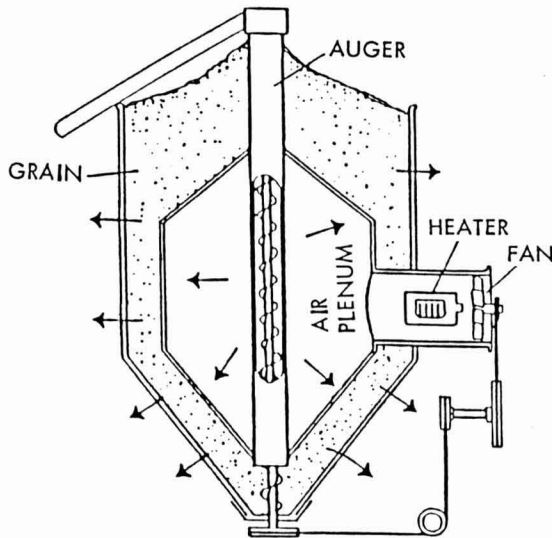
FIG. 1. CROSSFLOW CYLINDRICAL DRIER

These models were successful in predicting grain drying for a rectangular bed of grain. The models were not applied to radial dryers. In this paper a simplified mathematical model is proposed to describe the state of grain and air in a crossflow radial drier. The solution of the model for a crossflow configuration is simplified by adapting an easier solution technique used for the concurrent flow configuration. The model is validated using laboratory experimental data.

MODEL DEVELOPMENT

Figure 2 shows a sketch of the circular section of the dryer. To model the drying process, the grain chamber is divided into a number of circular control volumes. A typical control volume is shown in Fig. 2. Upon entering into each control volume, grain exchanges heat with the moving hot air. The heat exchange consists of the sensible heat $dq_s(r)$ and the latent heat $dq_l(r)$:

$$dq(r) = dq_s(r) + dq_1(r) \tag{1}$$

Figure 3 shows that the directions of air flow and grain flow through the control volume can be assumed such that a crossflow is transformed into a concurrent flow. Grain moves from 1.1 to 2.1 and the outlet conditions at 1.1

$(tg_{11};M_{11})$ become the inlet conditions at 2.1. Simultaneously air moves from 1.1 to 1.2 and the exit conditions from 1.1 $(ta_{11};H_{11})$ become the initial conditions at 1.2.
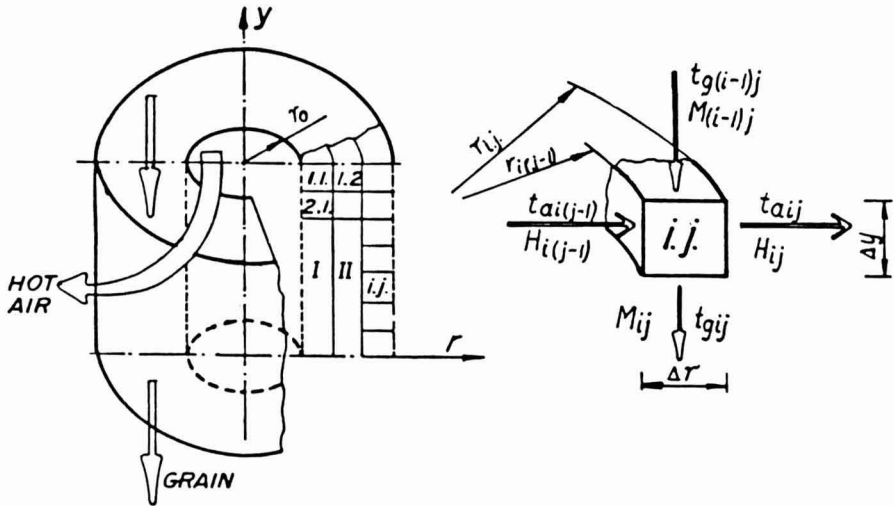
FIG. 2. A CROSS SECTION AND A SEGMENT OF THE GRAIN CHAMBER
AS CONTROL VOLUME
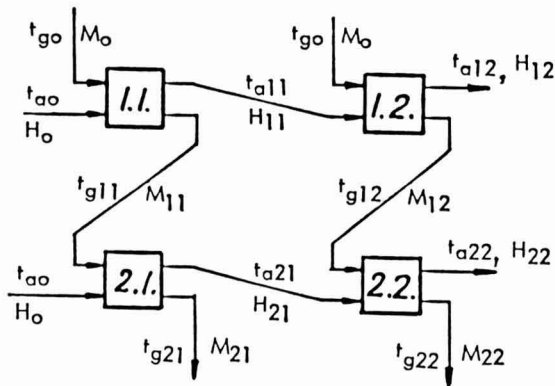
FIG. 3. MODELLING CROSSFLOW USING CONCURRENTFLOW PRINCIPLES

Heat and Moisture Balances

Consider the control volume shown in Fig. 4. For each radial element within the control volume the heat change of air can be written:

$$dq(r) = - v(r) \; A(r) \; c_a \; \rho_a \, dt_a(r) \tag{2}$$
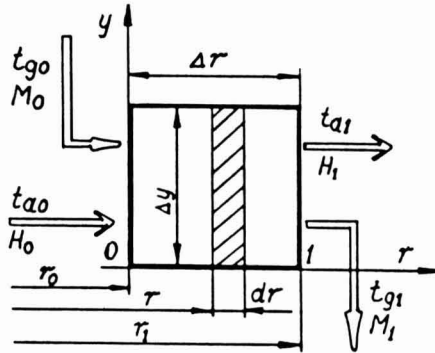
FIG. 4. DETAILS OF A CONTROL VOLUME

Assuming the air density remains constant over the control volume, the local values $v(r) \; A(r)\rho a$ can be replaced by the inlet values $v_0 A_0 \rho_a$.

$$dq(r) = - v_0 \; A_0 \; \rho_a \; c_a \; dt_a(r) \tag{2a}$$

where:

$$A_0 = 2\pi \; r_0 \, \Delta y$$

The change in the sensible heat of grain $dq_s(r)$ is expressed as:

$$dq_s(r) = - G \; c_g \; dt_g(r) \tag{3}$$

The sensible temperature differential between grain and air as they pass through the control volume is written as:

$$dt_a(r) - dt_g(r) = d\Delta t(r) \tag{4}$$

Using the definition of sensible heat ratio ψ given by Pabis (1971) for heating and drying again:

$$\psi = \frac{dq_s(r)}{dq(r)} , \tag{5}$$

and rearranging Eq. (2) and (3) and substituting in Eq. (4), yield:

$$-dq(r) \left(\frac{1}{A_0 \, v_0 \, \rho_a \, c_a} - \psi \, \frac{1}{G \, c_g} \right) = d\Delta t(r) \tag{6}$$

The net convective heat exchange in the control volume is written:

$$dq(r) = h_v \, 2\pi \, r \, dr \, \Delta y \, \Delta t(r) \tag{7}$$

Substituting Eq. (7) in Eq. (2), rearranging, and integrating over the control volume yield:

$$\int_{t_{a0}}^{t_{a1}} dt(r) = - \frac{h_v}{r_0 \, v_0 \, \rho_a \, c_a} \int_{r_0}^{r_1} \Delta t(r) \, r \, dr. \tag{8}$$

Substituting for $dq(r)$ from Eq. (7) in Eq. (6) and rearranging we get:

$$\int_{t_0}^{t_1} \frac{d\Delta t(r)}{\Delta t(r)} = - h_v \, 2\pi \, \Delta y \, m \int_{r_0}^{r_1} r \, dr, \tag{9}$$

where

$$m = \frac{1}{A_0 \, v_0 \, \rho_a \, c_a} - \psi \frac{1}{G \, c_g}. \tag{10}$$

Integrating Eq. (9) yields:

$$\Delta t_1 = \Delta t_0 \, \exp(- h_v \, \pi \, \Delta y \, m \, [r_1^2 - r_0^2 \,]). \tag{11}$$

Equation (11) can be written in a general form as:

$$\Delta t(r) = \Delta t_0 \, \exp(- h_v \, \pi \, \Delta y \, m \, [\, r^2 - r_0^2]). \tag{12}$$

Substituting Eq. (12) into Eq. (8) yields:

$$\int_{t_{a0}}^{t_{a1}} dt(r) = - \frac{h_v}{r_0 \, v_0 \, \rho_a \, c_a} \, \Delta t_0 \int_{r_0}^{r_1} \exp(- h_v \, \pi \, \Delta y \, m \, [r^2 - r_0^2]) \, r \, dr. \tag{13}$$

6

Using the following substitutions:

$$x = - h_v \, \pi \Delta y \, m \, [r^2 - r_0^2],$$ (13a)

$$dx = -2h_v \, \pi \Delta y \, m \, r \, dr,$$ (13b)

and

$$r \, dr = \frac{1}{-2 \, h_v \, \pi \Delta y \, m} \, dx$$ (13c)

in Eq. (13), we get:

$$\int_{t_{a0}}^{t_{a1}} dt(r) = - \frac{h_v}{r_0 \, v_0 \, \rho_a \, c_a} \, \Delta t_0 \int_{x_0}^{x_1} \frac{\exp(x)}{-2h_v \, \pi \Delta y \, m} \, dx$$ (13d)

Integrating Eq. (13d) yields:

$$t_{a1} - t_{a0} = \frac{\Delta t_0}{A_0 \, v_0 \, \rho_a \, c_a \, m} \, [\exp(x_1) - \exp(x_0)]$$ (13e)

where $x_1 = -h_v \, \pi \, \Delta y \, m \, (r_1^2 - r_0^2)$ and $x_0 = -h_v \, \pi \, \Delta y \, m \, (r_0^2 - r_0^2)$ at $r = r_0$ and $x_0 = 0$.

The final solution for air temperature will have the following form:

$$t_{a1} = t_{a0} + \frac{\Delta t_0}{A_0 \, v_0 \, \rho_a \, c_a \, m} \, [\exp(-h_v \, \pi \, \Delta y \, m \, (r_1^2 - r_0^2)) - 1]$$ (13f)

or

$$t_{a1} = t_{a0} - \frac{\Delta t_0}{2\pi \, r_0 \, v_0 \, \rho_a \, c_a \, \Delta y \, m} \, [1 - \exp(-h_v \pi \, \Delta y \, m \, (r_1^2 - r_0^2))]$$ (14)

Equation (14) is written for every (i,j) element as:

$$t_{aij} = t_{ai(j-1)} - \frac{t_{ai(j-1)} - t_{g(i-1)j}}{2\pi \, r_{(j-1)} v_{(j-1)} c_{aij} \Delta y \, m_{ij}} \, [1 - \exp(-h_{vij} \pi \, m_{ij} [r_j^2 - r^2_{(j-1)}])]$$ (15)

where

$$m_{ij} = \frac{1}{2\pi \, r_{(j-1)} \, v_{(j-1)} \rho_{aij} \, c_{aij} \Delta y} - \psi_{ij} \frac{1}{G_{ij} \, c_{gij}}$$ (16)

Similarly, the expression for the grain temperature at positions (i,j) will be:

$$t_{gij} = t_{g(i-1)j} + \psi_{ij} \frac{2\pi r_{(j-1)} v_{(j-1)} \rho_{aij} c_{aij} Y}{G_{ij} c_{gij}} [t_{ai(j-1)} - t_{aij}]$$

$$(17)$$

Determinations of the Sensible Heat Ratio

The sensible heat ratio ψ for heating grain is defined by the following numerical form:

$$\psi_{ij} = \frac{G_{ij} c_{gij} [t_{sij} - t_{g(i-1)j}]}{G_{ij} c_{gij} [t_{sij} - t_{g(i-1)j}] + G_{dij} \Delta M_{ij} h_{fg}}$$

$$(18)$$

The temperature of a spherical solid body can be described by a lump model provided the Biot Number, Bi, is less than 0.1:

$$t_s(\theta) = t_{a0} - [t_{a0} - t_{s0}] \exp(- \frac{6 h_{ij}}{c_g \rho_g d} \theta)$$

$$(19)$$

Equation (19) can be expressed throughout the drying chamber as follows:

$$t_{sij} = t_{ai(j-1)} - [t_{ai(j-1)} - t_{g(i-1)j}] \exp(- \frac{6 h_{ij}}{c_{gij} \rho_{gij} d_{ij}} \Delta\theta)$$

$$(20)$$

where

$$\Delta\theta = \frac{\Delta y \, \rho_b}{G_c}$$

$$(21)$$

The change in moisture content, ΔM_{ij}, is determined from an empirical thin layer drying equation.

The change in absolute humidity of air, H_{ij}, inside the drying chamber is determined from the mass balance:

$$H_{ij} = H_{i(j-1)} + M_{ij} \frac{G_{dij}}{2\pi \, r_{(j-1)} \, v_{(j-1)} \, \Delta y \, \rho_{aij}}$$

$$(22)$$

Equations (15), (17), (22), and a suitable thin-layer drying equation simulate the drying process in a radial dryer.

SOLUTION TECHNIQUE

The following assumptions were made to simplify computations:

(1) Constant values are assumed for the following parameters: the equivalent diameter of grain d, specific heat of air c_a, and the density of air ρ_a.
(2) Radial air distribution is uniform along the grain chamber.
(3) Grain flow is plugflow along the grain chamber.

For corn drying, thin-layer drying equation proposed by Troeger and Hukill (1971) and the equilibrium moisture content M_e developed by Kalchik et al. (1979) were used.

For wheat drying, the following form of thin-layer drying equation was used:

$$dM/d\Theta = -k(M - M_e) \tag{23}$$

The values of k and M_e for wheat were taken from Nellist (1978). The volumetric heat transfer coefficient h_v developed by Strumillo (1975) using the modified Nusselt number proposed by Pabis (1967, 1982) was used. The latent heat of vaporization of water for moist wheat, h_{fg}, was taken from Gallagher (1951).

MODEL VALIDATION

The simulation model was validated using two different experimental dryers.

Fixed Bed Crossflow Dryer

In a fixed bed dryer, the grain bed is stationary and drying proceeds with time. In a moving bed crossflow dryer, the grain bed dries as it moves downward. Drying time (Θ) in a fixed bed is equivalent to the time taken for a bed of grain to move a distance of y in a crossflow dryer ($\Theta = y/v_g$, where v_g is the grain velocity). Based upon this similarity, we used a fixed bed dryer with a radial cross section to validate the simulation model for crossflow dryer (Fig. 5).

The laboratory dryer was ¼ segment of a cylindrical dryer with a height of 60 mm. Copper-constantan thermocouples were placed at three radial positions as shown in Fig. 5. The junction of a thermocouple was inserted in a small hole drilled in the kernel to measure continuously the grain temperature. The thermocouples were connected to a datalogger whose output was recorded every minute. In each row three thermocouples recorded air temperature and two thermocouples recorded grain temperature.

Prior to each drying experiment, the chamber was filled with moist grain. A 1 cm thick sponge was used to press against the grain to prevent air leakage at the
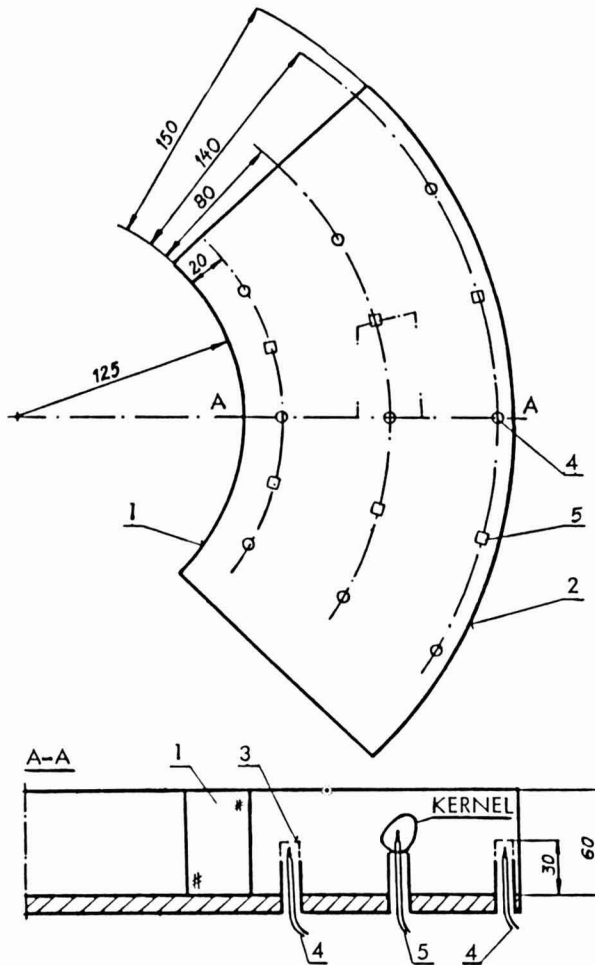
FIG. 5. DETAILS OF THE FIXED BED CROSSFLOW EXPERIMENTAL DRYER
1 - inner mesh
2 - outer mesh
3 - plastic tube
4 - ○ - air thermocouple
5 - □ - grain thermocouple

top. At a prescribed time interval, drying was stopped, grain samples were removed from inner, middle, and outer layers and the remaining grain was discarded. The chamber was refilled with grain of the initial moisture content of the previous test and another drying experiment was initiated. The drying process was continued longer than the previous test. This procedure was repeated seven times. Samples of dried grain after each experiment was kept separately in plastic bags. Each batch represented a different drying time. The moisture contents of samples were determined by the approved method (ASAE 1983).

Continuous Crossflow Dryer

In a separate experiment[1], a continuous crossflow cylindrical drier was used. Figure 6 shows a schematic view of this dryer. The dryer was constructed in two halves hinged at the bottom. The grain flow rate was adjusted by a discharge roller. The drying air temperature was measured by several thermocouples. Each of these thermocouples was positioned at different radial position. Five vertical strings were installed inside the drying chamber along which the thermocouples could move freely. Several grain kernels were fitted with thermocouple junctions embedded in them to measure the grain temperature. Five sets of these assemblies were placed radially in the drying chamber.
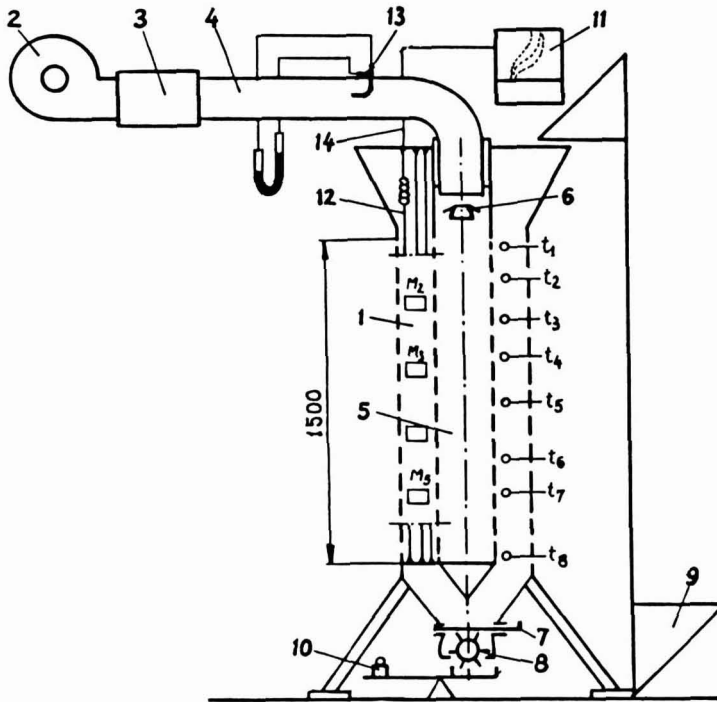
FIG. 6. DETAILS OF THE CONTINUOUS CROSSFLOW EXPERIMENTAL DRYER

1 - drying chamber	8 - discharge roller
2 - fan	9 - bucket elevator
3 - heater	10 - balance
4 - straight tubular duct	11 - temperature recorder
5 - inner perforated cylinder	12 - vertical strings
6 - air flow straightener	13 - averaging Pitot tube
7 - discharge gate	14 - grain thermocouples

[1]This experiment was performed in Poland by senior author.

The chamber was filled with freshly harvested grain and drying commenced. As grain moved downward, fresh grain was added at the top. After the initial top layer reached the bottom, the kernels having thermocouples in them were inserted at the top and were allowed to move downward with the grain mass. Drying stopped after the top layer reached the bottom. The two halves were separated and grain samples from four levels along the dryer height and at three layers (inner, middle, outer) were taken.

Fourteen tests were performed with the grain moisture content ranging from 0.37 to 0.60 dry basis. Drying air temperature was kept constant at 40 °C. One test from these experiments was selected to compare the simulation results. Data used for simulation are presented in Table 1. The experimental data for other tests have been published elsewhere (Cenkowski 1985).

TABLE 1.
DATA FOR THE SIMULATION

			fixed bed	cross-flow
			wheat	corn
Ambient air - t_{am}		[°C]	24.0	2.8
Drying temperature - t_{a0}		[°C]	62.0	41.0
Air velocity	v_0	[m/s]	0.08	0.10
Grain initial temp.	t_{g0}	[°C]	42.0	12.5
Grain moisture cont.	M_0	[kg/kgd.b]	0.320	0.350
Grain bulk density	ρ_b	[kg/m³]	800	620
Grain density	ρ	[kg/m³]	1400	1130
Wet grain flow rate	G_c	[kg/(m²h)]	533	426
Grain porosity	ϵ	[-]	0.43	0.45
Grain equivalent diameter d		[m]	0.004	0.008
Grain shape factor	ϕ	[-]	1.10	1.05
Height of the drier	h	[m]	1.5	1.5
Radius of the inner cylinder r_0		[m]	0.125	0.125
Thickness of the layer $\Delta r = \Delta y$		[m]	0.02	0.03

DISCUSSION

Figures 7 and 8 show the simulated and experimental temperatures of air and wheat in the fixed bed crossflow dryer during drying. The simulated temperatures were lower than the experimental temperatures. This might have been due to the simplifying assumption that grain temperature is uniform in the seed. Sokhansanj and Bruce (1987) showed that accurate grain temperatures can be predicted by using a condution model. Excessive heat losses from dryer may have been the reason the temperatures in the middle location (8 cm from inner mesh) showed a larger discrepancy.
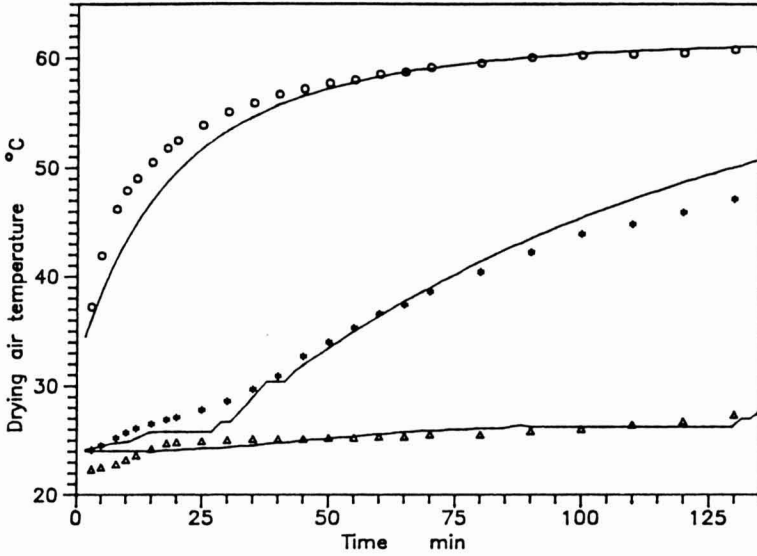
FIG. 7. EXPERIMENTAL AND SIMULATED AIR TEMPERATURES AT THREE
LOCATIONS IN THE FIXED BED CROSSFLOW DRYER DURING WHEAT DRYING
○ = 2 cm, * = 8 cm, △ = 14 cm from the inner screen.
--- = simulated
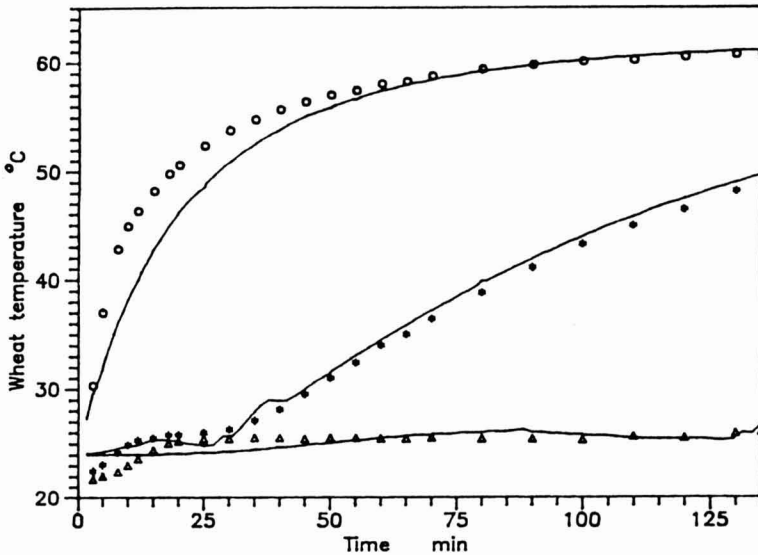
FIG. 8. EXPERIMENTAL AND SIMULATED WHEAT TEMPERATURES AT THREE
LOCATIONS IN THE FIXED BED CROSSFLOW CHAMBER DURING WHEAT DRYING
○ = 2 cm, * = 8 cm, △ = 14 cm from the inner screen.
--- = simulated

Figure 9 shows corn temperatures at three radial locations in the continuous crossflow dryer as grain travels downward. Experimental and simulated temperatures do not agree as well as the ones in Fig. 8. Part of the discrepancy may have been due to the uncertain location of the actual grain mass with respect to thermocouples. The experimental and theoretical temperatures at the middle location agreed better than those in the fixed-bed crossflow unit because of the larger size of the former one. The mean overall difference between the predicted and experimental temperature was 1 °C.
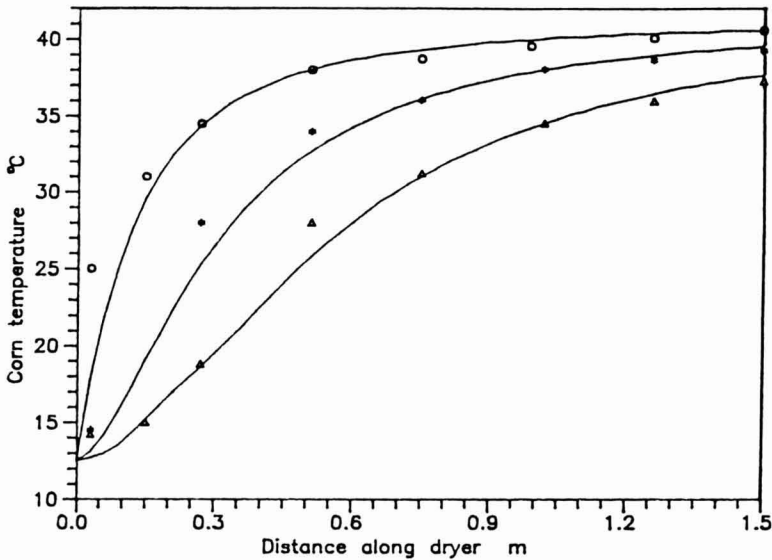
FIG. 9. EXPERIMENTAL AND SIMULATED GRAIN TEMPERATURES AT THREE LOCATIONS IN THE CROSSFLOW CONTINUES DURING CORN DRYING
○ = 3 cm, * = 6 cm, △ = 9 cm from the inner screen.
--- = simulated

Figure 10 and 11 show the moisture content of grain at three locations in the experimental dryers. In Fig. 10, the model predicted drying rate of the first layer reasonably well down to moisture content of about 14%. Beyond that point the model predicted lower moisture content which is a characteristic of the lump newtonian model (Eq. 23) used as the thin-layer drying equation.

Figure 11 shows the simulated and experimental moisture contents as corn moves downward in the continuous crossflow dryer. The experimental points shown in this figure indicate that the simulated moisture contents agree reasonably with the predicted values. The thin-layer drying model used for corn drying simulation covers a wide range of moisture contents. The difference between the experimental and the simulated moisture contents of grain for the middle layer was less than 0.3% moisture content w.b. The lower moisture contents
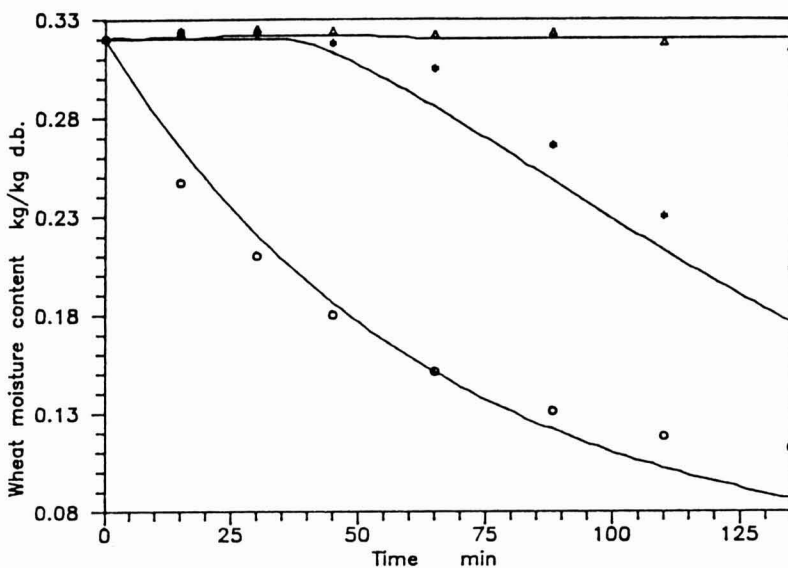
FIG. 10. EXPERIMENTAL AND SIMULATED WHEAT MOISTURE CONTENT
AT THE THREE LOCATIONS IN THE FIXED BED CROSSFLOW CHAMBER
$\bigcirc$ = 2 cm, * = 8 cm, $\triangle$ = 14 cm from the inner screen.
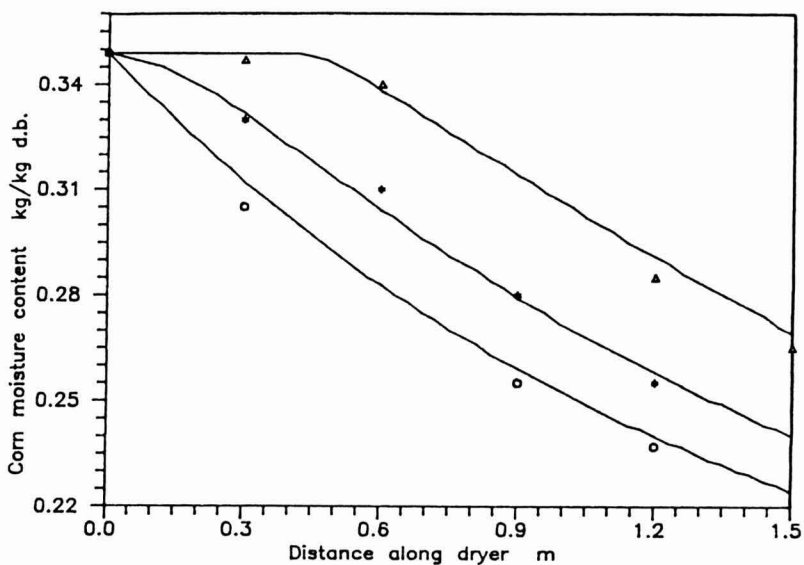
FIG. 11. EXPERIMENTAL AND SIMULATED CORN MOISTURE CONTENT AT THREE
LOCATIONS IN THE CONTINUOUS CROSSFLOW CYLINDRICAL DRIER
$\bigcirc$ = inner layer, * = middle layer, $\triangle$ = outer layer.

of the inside and outside layers may have been due to the heat conduction between wall and the grain which affected the drying rate.

SUMMARY AND CONCLUSIONS

Grain drying in radial continuous crossflow dryers was simulated by adapting equations describing the concurrentflow drying. The simulated air and grain temperatures and moisture contents were compared to the experimental data of drying wheat and corn; the agreement was good. The mean value of temperature discrepancy was 1 °C, and mean value of discrepancy for moisture content was 0.3% w.b. We conclude that the developed model facilitates the simulation of internal recirculating crossflow dryers that have a radial cross section.

LIST OF SYMBOLS

A = area m^2

c = specific heat capacity   kJ/(kg K)

d = diameter of particle   m

G = wet grain flow rate in the elementary section   kg/s

G_c = wet grain flow rate   kg/(m² h)

G_d = dry weight grain flow rate in the elementary section   kg/s

h = average surface heat transfer coefficient   kJ/(m² K h)

h_{fg} = latent heat of vaporization of water from moist grain kJ/kg

h_v = average volumetric heat transfer coefficient   kJ/(m³ K s)

H = humidity of drying air $kgH_2O/kgd.a.$

k = drying constant   1/min

M = grain moisture content $kgH_2O/kgd.m.$

r = radius of the drier column   m

rh = relative humidity   decimal

t = temperature   °C

v = velocity   m/s

ϵ = porosity of grain   decimal

ρ = density   kg/m³

Θ = time   s, h

Δ = increment

ψ = sensible heat ratio   decimal

Subscripts

a = air
b = bulk
d = dry
e = equilibrium
g = grain
i,j. = position index of elementary volume
0 = initial
s = sphere which has a grain dimension

REFERENCES

ASAE Standard. 1983. Moisture measurement — grain and seeds. S352. Agricultural Engineers Yearbook.

BAKKER-ARKEMA, F.W., LEREW, L.E., DE BOER, S.E. and ROTH, M.G. 1974. Grain drying simulation. Research Report No. 224. Michigan State University.

BRUCE, D.M. 1984. Simulation of multi-bed, concurrent-, counter-, and mixed-flow grain driers. J. Agric. Eng. Res. *30*, 361–372.

CENKOWSKI, S. 1985. Modelowanie procesu suszenia ziarna zboz - Cz. II. (Modelling of grain drying process - Part II). Zesz. Nauk. WSI w Opolu. z.8, Nr kol.112/1985, 75–94.

GALLAGHER, G.L. 1951. A method of determining the latent heat of agricultural crops. Agric. Eng. *32*(1), 34–38.

KALCHIK, S., SILVA, J. and BAKKER-ARKEMA, F.W. 1979. Engineering-economic comparison of five drying techniques for shelled corn on Michigan farms. ASAE Paper No. 79-3518.

NELLIST, M.E. and DUMONT, S. 1978. Desorption isotherms for wheat. Dep. Note DV/CDV/983/06010. NIAE Silsoe (unpubl.).

O'CALLAGHAN, J.R., MENZIES, D.J. and BAILEY, P.H. 1971. Digital simulation of agricultural drier performance. J. Agric. Eng. Res. *16* (3), 223–244.

PABIS, S. 1967. Grain drying in thin layers. Paper No. 1/C/4. Presented during Symposium Aug. 12, 1967, Silsoe England.

PABIS, S. 1971. The convective drying of grain layer in counter-flow. Roczn. Nauk Roln. t.68 z.4-C, 651–667.

PABIS, S. 1982. Theory of convective agricultural crop drying. PWRiL. Warszawa.

SOKHANSANJ, S. and BRUCE, D.M. 1987. A conduction model to predict grain temperatures in grain drying simulation. Trans. ASAE, *30*, 1181–1184.

STRUMILLO, Cz. 1975. Foundation of theory and drying technique. WNT Warszawa.

TROEGER, J.M. and HUKILL, W.V. 1971. Mathematical description of the drying rate of fully exposed corn. Trans. ASAE. (14):1153–1156, 1162.

THOMPSON, T.L., PEART, R.M. and FOSTER, G.M. 1968. Mathematical simulation of corn drying — a new model. Trans. ASAE 582–586.

PARTICULATE HEAT TRANSFER TO CANNED SNAP BEANS IN A STERITORT

C.L. FERNANDEZ[1], M.A. RAO[2] and S.P. RAJAVASIREDDI

Department of Food Science and Technology
Cornell University
Geneva, NY 14456

and

S.K. SASTRY

Department of Agricultural Engineering
The Ohio State University
Columbus, OH 43210

ABSTRACT

Convective heat transfer coefficient at the fluid-particle interface was determined for cut green beans in 303 × 406 cans processed in an agitated retort (FMC Steritort) by measuring the temperature of an aluminum bean and that of the surrounding Newtonian fluid. Four retort reel velocities, two sizes of aluminum beans, and six particle/fluid ratios were employed. Several correlation forms were tested. A correlation was developed in terms of the j-factor, Reynolds number (Re), and shape factor with an R^2 of 0.785. The particle's shape was a critical factor in the heat transfer correlations. The fluid-particle heat transfer rate increased with an increase in rotational velocity of the retort.

INTRODUCTION

Physical methods of preservation are widely used by the food industry. Canning has been one of the most widely used methods of food preservation. The annual production of canned foods in the USA is about 33 billion pounds (Lopez 1987). The American canning industry is made up of more than 1,500 plants (Jackson 1979) and produces many products.

---

[1]Currently at: Frigobras Lia Brasileira de Frigorificos, P.O. Box 6558, 05093, Sao Paulo, Brazil
[2]Address correspondence to author Rao.

The FMC Sterilmatic continuous pressure retort is widely used in the food industry. The advantages of agitated and continuous retorts include increase in production rate, reduction in floor space because fewer auxiliary equipment are required, reduction in steam and cooling water caused by regeneration, and reduction in labor requirements.

Heat transfer to liquid foods occur mainly by convection. The heating rate during convection heating can be improved by agitation which promotes mixing of the liquid. Besides agitation, other factors such as headspace also affect the heat transfer to liquids. A number of authors conducted studies on the can wall heat transfer coefficient in agitated retorts (Naveh and Kopelman 1980; Peralta-Rodriguez and Merson 1983; Javier *et al.* 1985; Anantheswaran and Rao 1985; Lenz and Lund 1978; Soule and Merson 1985; Duquenoy 1980; and Rao *et al.* 1985).

The rheological properties of a fluid being heated are important in the prediction of the heat transfer rates because they are highly correlated with the flow phenomena. Fluids can be classified according to their flow characteristics into two main classes: Newtonian and non-Newtonian. The former are those whose viscosity depends only on the temperature while the latter are those whose viscosity is dependent also on the shear rate and/or time (Rao 1986).

The Newtonian fluid behavior can be described by (Heldman and Singh 1981):

$$\tau = -\eta \, \dot{\gamma} \tag{1}$$

where τ is the shear stress, η is the coefficient of viscosity, and $\dot{\gamma}$ is the rate of shear. Some examples of Newtonian foods are milk, clear fruit juices, sucrose solutions and corn syrup (Rao 1986).

Particulate systems are very common amongst foods. Most of the studies on heat transfer in such systems have dealt with the effect of different factors on the heating rates of specific products processed in specific containers and retorts. However, there have been studies on modeling and heat transfer phenomena (DeRuyter and Brunet 1973; Manson and Cullen 1974).

Lenz and Lund (1978) studied heat transfer to spherical particulate systems processed in a Steritort. They determined the heat transfer coefficient at the particle-fluid interface which they found to be finite and not infinite in magnitude. A dimensionless correlation for particulate systems was developed in terms of Nusselt, Reynolds and Prandtl numbers, and of the ratio of bed volume to particle surface area. The heat transfer coefficient at the internal wall surface and the reel diameter as the characteristic dimension were used to estimate the dimensionless numbers.

Sastry (1984) used a similar procedure to study the heat transfer to whole mushrooms processed in a still retort. A dimensionless correlation was developed in terms of Nusselt, Prandtl and Grashof numbers because it was

assumed that in a still retort the convective heat transfer occurs by free convection. The correlation obtained, however, had a low magnitude of R^2 (0.327).

The overall objective of the present work was to study the heat transfer phenomena during the thermal processing of systems containing particles (cut green beans) surrounded by Newtonian fluids in an agitated retort (FMC Steritort). Specific objectives were to obtain data on heat transfer and to model the phenomena by means of dimensionless numbers based on the heat transfer coefficient at the particle-fluid interface, the product characeristics such as amount and size of the particles, the fluid properties and particle-fluid ratio, and the speed of rotation.

MATERIALS AND METHODS

In this work the effect of size of the particle, the ratio: mass of particle/mass of fluid, the thermal and physical characteristics of the fluid, and rotational velocities of the retort on the heat transfer rate of particulate systems were studied. In general, the procedures developed by Lenz and Lund (1978) for the determination of particle-fluid heat transfer coefficient were employed in the present study. The specific fluids, bean weights, and rotational speeds employed are summarized in Table 1.

TABLE 1.
VARIABLES USED IN THE EXPERIMENTS

Newtonian Test Liquids	Weight of Beans (g)	Rotational velocity (RPM)	Bean [a] size
Water	244 224 214	2 4	A2
Sugar s. 30%	204	6	
	184	8	A4
Sugar s. 60%	164		

[a]A2 aluminum bean weight 1.68 g, surface area 5.28 cm²,
A4 bean weight 5.63 g, surface area 10.77 cm².

Cut green beans were processed in 303 X 406 cans. The experiments were carried out in a Steritort (FMC Corp., San Jose, CA), which is a simulator of the Sterilmatic retort, a continuous retort used commercially. The Steritort has a revolving reel on which the cans are located. Each rotation consists of three distinct stages. When the can is in the upper part of the reel it only rotates about the reel axis and the agitation is not very intense. In the lower part of the reel the

can rotates around its own axis. The third part of the cycle is made up of the transition regions between the two prior parts.

Experimental Variables. The heat transfer in a particulate systems depends upon the size, shape and amount of particles present in the can (Manson and Cullen 1974). The present work deals with the effect of the size and amount of particles in the system. To evaluate these effects two aluminium beans and six particle/fluid ratios were used. The amount of beans were held constant (244 g. 224 g, 214 g, 204 g, 184 g, and 164 g) but the liquid amount varied a little from run to run because the headspace was fixed at ¼ in. (0.64 cm) and the densities of the liquids were different. The headspace was fixed because its important role in pure liquid systems processed in agitated retorts has been demonstrated (Naveh and Kopelman 1980) and it also was expected to occur with particulate systems. However, the effect of different magnitudes of headspace on heat transfer was not studied in this work. In order to study the effect of the rotational velocity on the heat transfer coefficient at the particle/fluid interface, four different speeds of rotation were used: 2, 4, 6, and 8 RPM.

The thermal and physical characteristics of the fluid also affect the heat transfer rate. Water and sugar solutions (30% and 50%) were used as the test fluids in order to cover reasonable ranges of their physical and thermal properties and consequently obtain reasonable range of magnitudes of dimensionless groups. It was observed that some dilution of the sugar solutions occured after the liquid was in contact with the thawed beans in the can for a few minutes. For these reasons the °Brix of the solution was measured after the liquid was filled and allowed to rest for about 5 min. On the average these concentrations changed from 30% and 60% to 21% and 50.9%, respectively.

Physical and thermal properties of the solutions at the final concentration were evaluated at 65 °C, the bulk temperature, using a computer program developed by Anantheswaran (1984). The program computed the properties at a selected temperature and it was based on data taken from the literature sources cited in Anantheswaran and Rao (1985) and Fernandez (1987). The use of properties evaluated at a single temperature was based on the work of Anantheswaran (1984), and Rao et al. (1985). Briefly, the reasons are: (1) during the experiment, the temperatures of the bulk of the fluid and that of the aluminum bean are changing continuously with time, (2) as a consequence, one has to evaluate the fluid properties and the pertinent dimensionless groups either at one representative temperature or at many temperatures that are encountered from the beginning to the end of a test, (3) Lenz and Lund (1978) evaluated the properties at the retort temperature in their correlation of container wall heat transfer coefficient, but we (Anantheswaran 1984; Rao et al. 1985) selected 65 °C because it represented the average bulk temperature in the can during a test, and (4) in the

present study, we decidied to first try dimensionless correlations based on physical and thermal properties at 65 °C and the results, as will be seen later, were satisfactory.

Experimental Procedure

Frozen green beans, obtained from a local processor were used in the experiments. They were at −10 °C and thawed in distilled water about one hour before the start of a run.

In order to estimate the heat transfer coefficient at the particle-fluid interface, the temperature of the fluid and the internal temperature of an aluminum bean placed in the can were recorded. Figure 1 represents the apparatus used to measure the temperatures. Two needle type thermocouples (Type CNS, Ecklund Custom Thermocouples, Cape Coral, FL) were introduced into each can. The thermocouple measuring the bean temperature (bean thermocouple) was introduced in one end of the can and was attached to an Aluminum bean fixed by a small amount of rubber cement. Aluminum was used because this material has low heat transfer resistance with the anticipated surface heat transfer resistance allowing the assumption that the whole particle is at a uniform temperature, the surface temperature, at a given time. The other thermocouple was introduced in the other end of the can to measure the fluid temperature. We noted that Lenz and Lund (1978) employed lead spheres in their study of particle-fluid heat transfer for the same purpose.
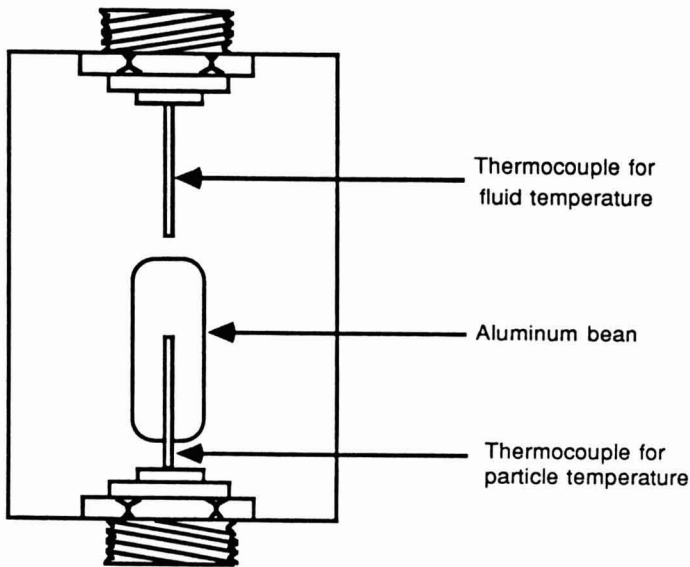
FIG. 1. SCHEMATIC OF THE THERMOCOUPLES TO MEASURE
TEMPERATURES OF THE BEAN AND FLUID

After the bean thermocouple was installed and the Aluminum bean was fixed, the can was filled with cut green beans followed by the test fluid up to a headspace of 1/4 in. (0.64 cm). The can was then closed and placed in the Steritort. The cans were processed at 240°F (115.6°C). The particle and fluid temperatures were recorded every 10 s using a datalogger (Digistrip III, Kaye Instruments, Bedford, MA). The data were stored on floppy disks of a microcomputer (Apple II+, Apple Computer Inc., Cupertino, CA) and transferred to a mainframe computer (Prime 9750).

The time-temperature data were analyzed and the heat transfer coefficients were calculated using a computer program (Sastry 1984) that was based on the scheme developed by Lenz and Lund (1978) to solve the heat balance equation:

$$m_p \, C_p \, \frac{d \, T_p}{dt} = - \, h_p \, A_p \, (T_p - T_f) \tag{2}$$

In Eq. (2), h_p is the heat transfer coefficient at the particle-fluid interface, T_f is the fluid temperature, and m_p, C_p, T_p, and A_p are the mass, specific heat, temperature, and area of the aluminum particle, respectively. Equation (2) was solved on a Prime 9750 digital computer using a fourth order Runge-Kutta procedure starting from the initial temperature value and using a range of trial h_p values. The trial value of h_p that yielded the lowest sum of squares of the difference between the experimental and predicted values of temperatures was used as the representative heat transfer coefficient.

Dimensionless numbers were calculated and correlations among them developed using the statistical package Minitab (Pennsylvania State University, State College, PA). Additional details of the materials and methods, as well as the data analyses can be found in the thesis of Fernandez (1987).

RESULTS AND DISCUSSION

Typical profiles of the fluid and the particle temperatures are presented in Fig. 2. Initially, the particle and fluid temperatures are the same at the beginning of the heating period. During the first part of the heating period the particle temperature was lower than that of the fluid due to the heat transfer resistance at the particle surface. As the fluid and the particle temperatures approached the retort temperature (115.6°C), the difference between them decreased and the two temperatures were equal.

The difference in temperatures during the first period of the heating was used to estimate the heat transfer coefficient at the particle - fluid interface. A difference of 1°C was set as the minimum acceptable in order to standardize the data used in the heat transfer coefficient calculations. For this reason the number of time - temperature points varied from run to run.
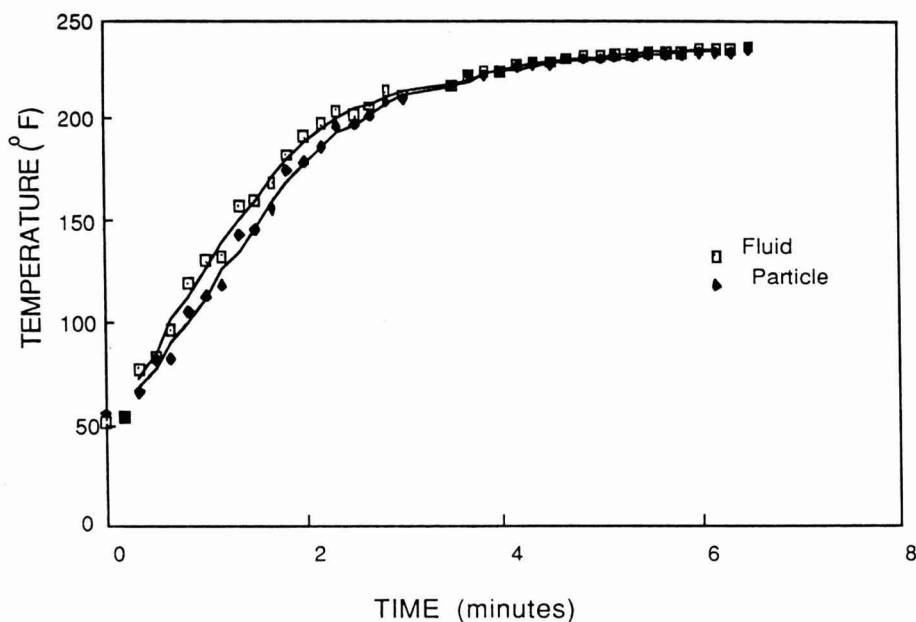
FIG. 2. HEATING CURVE OF NEWTONIAN FLUID

Regression analyses were carried out in order to obtain an equation correlating the dimensionless groups to model heat transfer to particulate systems. Ninety-four observations were used to develop the dimensionless correlations for the tested fluids. Table 2 contains the correlations obtained using Re, Stanton, and the Colburn j-factor and their R^2. Because considerable effort was spent on studying the role of various dimensionless groups and their arrangement, they will be described in detail.

Determination of Characteristic Dimension

The first attempt was to determine the characteristic dimension that should be used in the correlation in order to better correlate the data. Two dimensions were used: the bean diameter under the assumption that free convection was significant in the process (Anantheswaran and Rao 1985) and the reel diameter under the assumption that forced convection was the most important heat transfer mechanism occurring in the system (Lenz and Lund 1978).

Correlations where Nusselt number (Nu) was a function of the Reynolds (Re), Prandtl (Pr) or the product of Pr with the Grashof (Pr Gr) numbers, and the ratio of the viscosity at bulk temperature to the viscosity at wall temperature were developed using both the reel diameter and the bean diameter as the

TABLE 2.
CORRELATION FORMS TESTED AND THEIR R^2

$Nu = 0.861 \ Re^{0.55} \ Pr^{0.17} \ (\eta_b / \eta_w)^{1.19}$ $R^2 = 0.324$

$Nu = 1.5 \times 10^{-4} \ Re^{0.264} \ (Gr \times Pr)^{0.583} \ (\eta_b / \eta_w)^{2.79}$ $R^2 = 0.550$

$Nu = 0.81 \ Re^{0.551} \ Pr^{0.01} \ \varepsilon^{0.087} \ (\eta_b / \eta_w)^{1.62}$ $R^2 = 0.324$

$Nu = 1.2 \times 10^5 \ Re^{0.262} \ Pr^{1.28} \ \Omega^{7.28} \ (\eta_b / \eta_w)^{-2.90}$ $R^2 = 0.568$

$St = 3.6 \times 10^4 \ Re^{-0.728} \ Pr^{-0.697} \ \Omega^{7.11}$ $R^2 = 0.516$

$St_c = 1,300 \ Re_m^{-0.628} \ Pr^{-0.473} \ \Omega^{6.09}$ $R^2 = 0.399$

$St_m = 5.4 \times 10^4 \ Re_m^{-0.736} \ Pr^{-0.722} \ \Omega^{7.25}$ $R^2 = 0.534$

$j = 26,900 \ Re^{-0.706} \ \Omega^{6.98}$ $R^2 = 0.785$

$j_m = 36,300 \ Re_m^{-0.696} \ \Omega^{0.701}$ $R^2 = 0.766$

$j = 36,300 \ Re^{-0.728} \ Pr^{-0.03} \ \Omega^{7.11}$ $R^2 = 0.785$

$j_m = 54,200 \ Re^{-0.736} \ Pr^{-0.055} \ \Omega^{7.24}$ $R^2 = 0.767$

---

[a]St is Stanton number defined by Eq. 6; St_c Stanton number defined by Eq. 4; St_m is Stanton number defined by Eq. 6 but using modified Reynolds number defined by Eq. 5; jm denotes j-factor with modified Reynolds number. In the first four equations, η_w was evaluated at retort temperature.

characteristic dimension. The magnitudes of R^2 obtained when the bean diameter were used (30–50%) were higher than those obtained when the reel diameter was used (18–35%). Therefore, the bean diameter was chosen to be used in the following analysis.

The correlation forms consisting of Nu, Re, and Pr (or Pr Gr) were used to determine whether void volume, shape factor, and viscosity ratio need to be considered.

Role of Void Volume, Shape Factor, Viscosity Ratio

The amount of the particles, or the ratio: mass of particles/mass of fluid, has been presented in the literature as a critical factor affecting heat transfer to particulate systems. Thus, the void volume (ratio of liquid volume to the can volume) was added to the correlation in order to account for the influence of the amount of particles. The addition of the void volume to the dimensionless groups did not significantly improve the magnitude of R^2. Furthermore, the Student t-ratio (value of the coefficient divided by its standard deviation) of the void volume was below the cutoff point for 5% confidence level. Hence, this term was discarded.

The shape of the particle was also expected to significantly affect the heat transfer to particulate systems. The shape factor, defined as the ratio of surface area of a sphere of volume equal to that of the particle to the surface area of the particle (Foust et al., 1980), was added to the dimensionless groups. It is expressed as:

$$\Omega = \frac{\pi \left(\dfrac{6\, V_p}{\pi} \right)^{\frac{2}{3}}}{A_p} \tag{3}$$

where V_p is the particle volume and A_p is the particle surface area was added to the dimensionless groups. The addition significantly increased the R^2 of the correlations (56%). Moreover, the Student t-ratio of the shape factor term was always very high, implying that its coefficient was different than zero. Hence, it was concluded that the particle's shape is a critical factor affecting the heat transfer to particulate systems and a term accounting for its influence should be present in the correlation.

In all correlations developed, the ratio of the viscosities was highly correlated to the Pr number. Thus, the coefficient of this term was assumed as being zero and was discarded from further analysis.

Modeling the System as a Fluidized Bed

The R^2 of the correlations with Nu as the dependent variable were low even when the shape factor was present (0.58) The system being studied can be approximated by a two-phase fluidized bed. Thus, the dimensionless groups used to model heat transfer to fluidized beds should be suitable to describe canned particulate systems.

Chiu and Ziegler (1985) studied the heat transfer to fluidized beds. They used a modified Stanton number defined as:

$$St_c = \frac{h\,\varepsilon}{\rho\, C_p\, v} \tag{4}$$

and a modified Reynolds number defined as:

$$Re_m = \frac{v\,\rho}{S\,(1-\varepsilon)\,\eta} \tag{5}$$

where S is the surface area of the particle per unit of volume and ϵ is the void volume of the system. The St number is also defined as the Nu number divided by Re and Pr numbers (Foust et al., 1980):

$$St = \frac{Nu}{Re\, Pr} \tag{6}$$

Correlations were developed where St number was a function of Reynolds and Pr numbers, and shape factor. Three different St numbers were used: the form (Eq. 4) used by Chiu and Ziegler (1985), and the form defined by Eq. 6 using both the Reynolds number (Re) used previously, and the modified Reynolds number, defined by Eq. 5. However, the use of the St number did not improve the R^2 of the correlations. In fact they decreased, but were in the same range of the ones from correlations using Re number, i.e., about 50%.

Correlations using the St number defined by Eq. 6 had slightly higher R^2 than those using the modified (St_c) number used by Chiu and Ziegler (1985). It is of interest to note that the correlations using St number presented negative exponent for the Re and Pr numbers. Both Re and Pr, however, are present in the denominator of the St number, so that when St number is expanded in terms of Nu, Re, and Pr numbers they have positive exponents. Chiu and Ziegler (1985) also obtained negative exponents for Reynolds and Pr numbers.

Modeling the System as a Packed Bed

Another alternative was to treat the system as a packed bed using the same dimensionless numbers employed to model the heat transfer to these systems. The Colburn j-factor has been used in empirical correlations to describe heat transfer to packed beds. It is defined as:

$$j = \frac{Nu\,Pr^{\frac{2}{3}}}{Re\,Pr} \tag{7}$$

Bird et al. (1960) presented two correlations for heat transfer in packed beds, one for Re numbers lower than 50 and another for Re numbers higher than 50, where the Colburn j-factor was a function of the Re number and the shape factor.

Correlations where j-factor is a function of the Re number and shape factor were developed having either the Re number or the modified Reynolds number (Eq. 5). The magnitudes of R^2, about 70%, obtained for these correlations were much higher than those obtained when either Re or St numbers was used as the independent variable. Thus, the assumption that this system can be treated as a packed bed was acceptable.

When the Pr number was also included in the correlation the magnitude of R^2 did not increase. Moreover, the Student t-ratio of the Pr number was below the 5% cutoff point. The term accounting for the natural convection of the system (PR Gr) was also included, but it did not significantly improve the R^2. The t-ratio of this term was also below the 5% cutoff point.

The correlation:

$$j = 26{,}900\,Re^{-0.706}\,\Omega^{6.98} \tag{8}$$

was the one that best described the heat transfer rates. Table 3 contains the range
of the dimensionless groups used in this work.

Equation 8 is similar to that presented by Bird et al. (1960) for heat transfer in
packed beds. However, the magnitude of the exponents and the constant are dif-
ferent. In their correlation the Re number exponent is equal to -0.51 (Re $<$ 50)
and the shape factor exponent is equal to one. In particular, the exponent of the
shape factor in the present study is much higher than that presented by Bird et al.
(1960). This difference in the magnitude of the exponent is because the present
system is not exactly a packed bed. The high exponent for the shape factor term
indicates that it is a critical factor affecting the heat transfer in the system. This is
due to the fact that the shape of the particle influences the flow of the liquid in the
system.

Figure 3 shows the plot of the experimental data and the predicted line accor-
ding to Eq. 8. It can be seen that there is a good alignment between the ex-
perimental and predicted data. The line obtained had a correlation coefficient of
0.90 which shows that Eq. 8 models the present complex particulate system very
well.
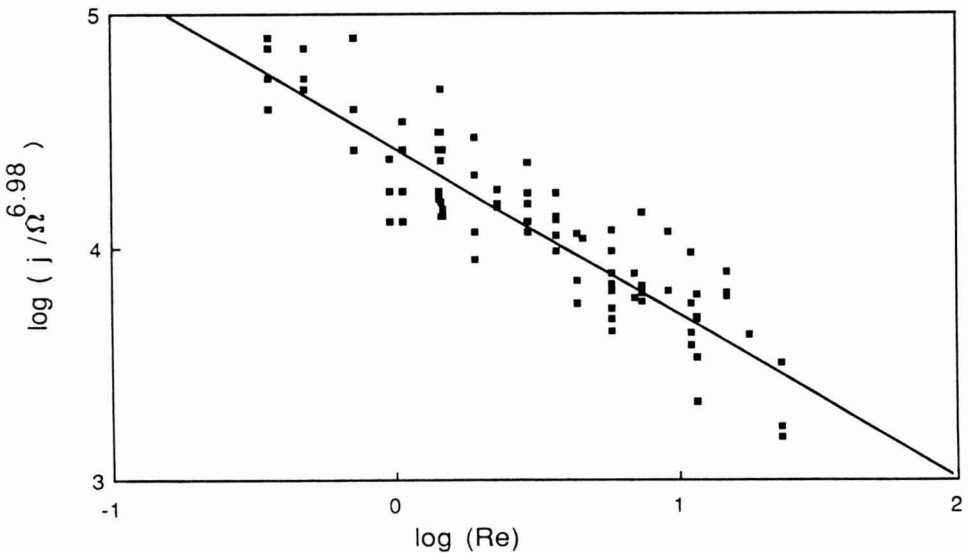
FIG. 3. GRAPHICAL CORRELATION BETWEEN DATA OBSERVED
AND PREDICTED FOR NEWTONIAN FLUIDS

Figure 4 presents the response surface for the j-factor predicted by Eq. 8 as a
function of Re number and shape factor. The increase of the Re number resulted

in decrease of the j-factor. This fact does not mean that an increase in the rotational velocity results in decrease of the heat transfer rate because the velocity term is in the denominator of the j-factor. Equation 8 can be written as:

$$Nu = 2.7 \times 10^4 \, Re^{0.294} \, Pr^{0.33} \, \Omega^{6.98} \qquad (9)$$

From Eq. 9 it can be seen that although the increase of the rotational velocity results in decrease of the j-factor, the heating rate increases because the Re number increases. An increase in the magnitude of the shape factor, in other words as we approach the shape of a sphere, results in increase of the j-factor and the heat transfer rate. In the response surface it can be seen that the increase is much more intense when the Re number is small. It is of interest to note that, although the Pr number is not seen in the correlation, it is present as part of the j-factor.

$$j = 2.7 \times 10^4 Re^{-0.706} \Omega^{6.98}$$
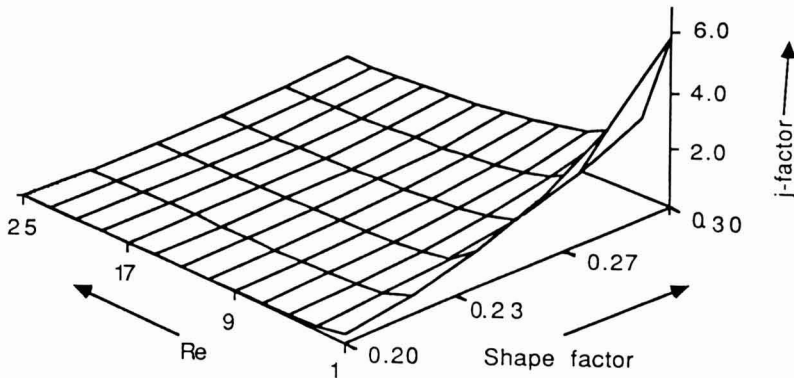
FIG. 4. RESPONSE SURFACE FOR j-factor FOR NEWTONIAN FLUIDS

CONCLUSIONS

Canned particulate matter processed in an agitated retort is a very complex system. The analysis of the influence of the different variables (speed of rotation, shape of the particle, amount of particle, and fluid characteristic) was done through regression analysis of dimensionless groups.

The Colburn j-factor, used to model heat transfer in packed beds, was used to model the heat transfer occurring in the system containing a Newtonian fluid as

the liquid phase as a function of Reynolds number and of shape factor. The particle diameter was used as the characteristic dimension.

The shape of the particle was a critical factor so that the exponent of this term was high. As the particle shape approached the shape of a sphere, the rate of heat transfer increased. This is due to the fact that the shape of the particle affected the formation of the ducts where a fluid flows, affecting the flow of the liquid and, consequently, the heat transfer coefficient at the particle-fluid interface.

An increase in rotational velocity of the retort resulted in increase in the heating rate and its influence was expressed in terms of the Reynolds number whose magnitude increased with the velocity increase.

Although correlations with high R-square were obtained, more research is needed to confirm these correlations. Other particle shapes and sizes should be studied in order to confirm the strong effect of the particle shape found in this work. The influence of the size of the container and the headspace were neglected in this study. They should also be studied in further works. In particular, studies should be conducted with non-Newtonian fluids.

NOMENCLATURE

A_p - particle surface area m^2

C_p - specific heat   J/kg K

D - can or particle diameter   m

g - acceleration constant for gravity m/s^2

h - heat transfer coefficient $W/(m^2\ K)$

h_p - heat transfer coef. at the particle fluid interface $W/(m^2\ K)$

k - thermal conductivity $W/(m\ K)$

N - rotations per minute   rpm

S - radius of reel   m

T - temperature   K

T_f - fluid temperature   K

T_s - steam temperature   K

V_c - volume of the can m^3

V_p - volume of the particle m^3

β - coefficient of thermal expansion K^{-1}

ϵ - void volume   ---

γ - rate of shear s^{-1}

η - viscosity   Pa s

η_b - viscosity at the bulk temperature   Pa s

η_w - viscosity at the wall temperature   Pa s
Ω - shape factor   ---
π - 3.1415 ...   ---
ϱ - density   kg/m³
τ - shear stress   Pa

Dimensionless Groups:

$$Gr = \frac{D^3 g \, \beta \, \rho^2 \Delta T}{\eta^2} = \text{Grashof number}$$

$$j = \frac{Nu \, Pr^{\frac{2}{3}}}{Re \, Pr} = \text{Colburn j - factor}$$

$$Nu = \frac{h \, D}{k} = \text{Nusselt number}$$

$$Pr = \frac{C_p \, \eta}{k} = \text{Prandtl number}$$

$$Re = \frac{D^2 \, N \, \rho}{\eta} = \text{Reynolds number}$$

$$Re_m = \frac{v \, \rho}{A_p(1-\varepsilon) \, \eta} = \text{modified Reynolds number}$$

$$St = \frac{Nu}{Re \, Pr} = \text{Stanton number}$$

$$St_c = \frac{h\,\varepsilon}{\rho\,C_p\,v} = \text{Modified Stanton number used by Chiu and Ziegler (1985)}$$

$$St_m = \frac{Nu}{Re_m\,Pr} = \text{Modified Stanton number}$$

REFERENCES

ANANTHESWARAN, R.C. 1984. Heat penetration to model fluid foods in cans during end-over-end rotation. Ph.D. Thesis. Cornell University, Ithaca, NY. (University Microfilms, Intl., Ann Arbor, MI).

ANANTHESWARAN, R.C. and RAO, M.A. 1985. Heat transfer to model Newtonian liquid foods in cans during end-over-end rotations. J. Food Eng. *4*, 1–19.

BIRD, R.B., STEWART, W.E. and LIGHTFOOT, E.N. 1960. *Transport Phenomena*. John Wiley & Sons, New York.

CHIU, T.M. and ZIEGLER, E.N. 1985. Liquid holdup and heat transfer coefficient in liquid-solid and three-phase fluidized beds. AlCheE J. *31*, 1504–1509.

DE RUYTER, P.W. and BRUNET, R. 1973. Estimation of process conditions for continous sterilization of foods containing particles. Food Tech. *27*, 44–51.

DUQUENOY, A. 1980. Heat transfer to canned liquids. In *Food Process Engineering*, Vol. 1, (P. Linko, Y. Malkki, J. Olkku and J. Larinkari, eds.) pp. 483–489. Applied Science Publishers Ltd., Essex, England.

FERNANDEZ, C.L. 1987. Heat transfer to two-phase system processed in a Steritort. M.S. Thesis. Cornell University, Ithaca, NY.

FOUST, A.S., WENZEL, L.A., CLUMP, C.W., MAUS, L. and ANDERSEN, L.B. 1980. *Principles of Unit Operations*, 2nd ed. John Wiley & Sons, New York.

HELDMAN, D.R. and SINGH, R.P. 1981. *Food Process Engineering*, 2nd. ed. Van Nostrand Reinhold/AVI, New York.

JACKSON, J.M. 1979. Development of the canning industry. Ch. 1. In *Fundamentals of Food Canning Technology*, (J.M. Jackson and B.M Shinn, ed.) pp. 1–19. Van Nostrand Reinhold/AVI, New York.

JAVIER, R.A., NAVEH, D., PERLSTEIN, E. and KOPELMAN, I.J. 1985. Convective heating rate parameters of model solution in an agitating retort. Lebensm. Wiss. w-tech. *18*, 311–315.

LENZ, M.K. and LUND, D.B. 1978. The lethality-Fourier number method. Heating rate variations and lethality confidence intervals for forced convection heated foods in containers. J. Food Proc. Eng. *2*(3), 227–271.

LOPEZ, A. 1987. *A Complete Course in Canning*, Vol. 1, 12th ed. The Canning Trade, Baltimore, MD.

MANSON, J.E. and CULLEN, J.F. 1974. Thermal process simulation for asseptic processing of foods containing discrete particulate matter. J. Food Sci. *39*, 1084–1089.

NAVEH, D. and KOPELMAN, I.J. 1980. Effect of some processing parameters on the heat transfer coefficient in a retorting autoclave. J. Food Proc. Pres. *4*, 67–77.

PERALTA-RODRIQUEZ, R.D. and MERSON, R.L. 1983. Experimental verification of the heat transfer model for simulated liquid foods undergoing flame sterilization. J. Food Sci. *48*, 726–733.

RAO, M.A., COOLEY, H.J. and ENNIS, R.W. 1985. Convective heat transfer to canned liquid food in a Steritort. J. Food Sci. *50*, 150–154.

RAO, M.A. 1986b. Rheological properties of fluid foods. In *Engineering Properties of Foods*, (M.A. Rao and S.S. H. Rizvi, eds.). Marcel Dekker, New York.

SASTRY, S.K. 1984. Convective heat transfer coefficients for canned mushrooms processed in still retort. Paper No. 84-6517, presented at the 1984 ASAE Winter Meeting.

SOULE, C.L. and MERSON, R.L. 1985. Heat transfer coefficients to Newtonian liquids in axially rotated cans. J. Food Eng. *8*, 33–46.

WEAST, R.C. and ASTLE, M.J. 1980. *CRC Handbook of Chemistry and Physics*, (R.C. Weast and M.J. Astle, eds.) CRC Press, Boca Raton, FL.

STRENGTH CHARACTERISTICS OF PRESSURIZED CANS

PHILIP L. BREWBAKER[1]

University of California, Davis
National Food Processors
Berkeley, California 94710

and

JERALD M. HENDERSON[2]

Mechanical Engineering and Food Science and Technology
University of California, Davis 95616

ABSTRACT

To study the strength advantages of pressurized cans used for food packaging, two indicators of can strength, maximum axial load and maximum external pressure, were investigated experimentally. Unbeaded 303 × 406 steel cans having several thicknesses and tempers with various internal pressures were tested. Also tested were beaded steel cans and aluminum cans with 206 × 406 dimensions. Failure of the cans was by both buckling and yielding. The results indicated that steel can thicknesses could be significantly reduced, and beading eliminated, by using internal pressure to supplement can strength.

INTRODUCTION

In 1981, the U.S. food industry purchased about 30 billion cans, of which 96% were steel (Anon. 1981a). Those cans cost the food processors as much as or more than the cost of the product placed inside them (Anon. 1981b).

The high cost of cans is not new: The standard 3-piece tin plated, beaded steel can has been scrutinized by canmakers for decades for savings. New beading, tempering, side seaming methods, and the development of 2 piece steels cans have helped reduce these costs somewhat (McKernan 1983; Anon. 1981a). The use of alternative materials has also been examined.

An obvious way to save money is to put less material in each can. This usually reduces the thickness of the sidewall in the can. Another way is to use materials in the can which are not as strong as steel; very thin cans may be less expensive if made with aluminum rather than steel (Leonard 1980). The recent use of plastics in some food cans is also motivated by economics (Knill 1985). Using less material, and weaker, usually lighter materials saves on transportation costs as well. Of course, there is a practical limit to reducing sidewall thicknesses and using weaker materials. Past that limit cans will no longer withstand common usage without failure.

If it were possible to cause an internal pressure in a can, it would be possible to reduce the required material without sacrificing strength. When cans deform, they usually deform by decreasing the overall volume within the can. Such a decrease in volume is aided by the vacuum placed in most cans. A positive internal pressure, on the other hand, would react against this tendency.

Beer and soft drinks produce a pressure in the can by carbonation which significantly aids the strength of the can. These products can be packaged in relatively thin-walled aluminum cans because of the internal pressure.

A new technique which pressurizes the cans of noncarbonated products is now in commercial use on a limited scale (Frye 1984; Anon. 1982). The can is pressurized by injection of liquid nitrogen in controlled amounts into the headspace after product filling and just prior to the seaming operation. After seaming, evaporation of the nitrogen creates the necessary pressure. Because of this or some other new technology, pressurization may be possible with many canned products in the future. It is unclear, however, to what degree pressurization could be used to supplement the material strength of cans.

The purpose of this study was to test the strength of pressurized food cans, to compare them with cans currently being used, and to obtain an idea of how pressure could aid can strength, and by how much, that is, obtain an indication of what material and material thickness changes could be contemplated in cans if pressurization were to become a more popular processing option in the future.

MATERIALS AND METHODS

Can Strength

Two strength criteria important in common can failures were used in this study (Brewbaker 1986). *Load resistance* is the maximum axial load, in pounds, that a can will withstand before deforming significantly from its original configuration. The load is along the long axis of the can because most stacking loads occur along this axis. The load resistance, is a value that would relate directly to the amount of stacking load a particular can could take without failing.

Panel Resistance is the maximum external pressure, in psi, that a can will withstand before deformation. Panelling can also be caused by a concentrated load on the sidewall, nevertheless, this panel resistance test using external pressure is easily applied, the results are easily generalized, and the conclusions seem as applicable as any other approach.

Cans Studied

To measure the effect of a number of factors, primarily pressure, on can strength, a variety of cans were tested. See Table 1. All of the steel cans used in this study were of the 303 × 406 (16 oz) size. This allowed a direct comparison of the results without considering size; also, many food cans are of this size. The steel cans were the primary emphasis of this project, but a few aluminum cans of a similar size were included for comparative purposes; they were of the 206 × 406 (12 oz) size, because of availability.

To determine what can strengths are acceptable to food processors for the protection of their products, ten beaded steel cans were purchased from a local supermarket and tested directly for load resistance. These cans contained vegetables from Del Monte USA, San Francisco, CA. All were beaded, and eight of them were of three-piece, welded side seam construction. The other two were two-piece beaded cans. Forty cans from the National Steel Corporation, Pittsburgh, PA, were also tested in load resistance. These cans were empty, but were sealed. They were beaded three-piece cans with welded side seams from 75 lb base box weight tinplate, a common thickness in food cans. Ten of the cans were sealed under a vacuum of 10 in Hg, a common amount in canned foods. Ten of the cans were sealed at atmospheric pressure, ten were pressurized to 14 psi, and ten were pressurized to 20 psi before testing. For panel resistance, fifteen National Steel cans were sealed and tested.

The majority of this study involved testing unbeaded steel cans for several reasons. First, pressurizing cans would improve panel resistance greatly, hopefully enough to make beading redundant. Second, unbeaded cans gave an opportunity to study, in a single material and geometry, the effect of can temper, thickness, and pressure on strength, without the difficult geometrical considerations of beading. Third, an unbeaded three-piece can resembles closely a right circular cylinder. Analytical methods exist for this geometry that could be used to help understand can strength.

To this end, 800 unbeaded cans were manufactured by Wierton Steel, Wierton, West Virginia, for this project. These three-piece, welded side seam cans were essentially common 303 × 406 food cans without beading. Eight different cans (100 of each type) were obtained. The variables were thickness and temper (Table 1). The two tempers, DR8 and CAT4, are common tempers for can making tinplate. CAT4 tinplate has been continuously annealed, while DR8 has been

TABLE 1.
CANS TESTED

| Can Types | Sizes | Number of cans | | | Source |
| | | Load Resistance | | Panel | |
		Zero press	With press	Resistance	
Beaded Steel for strength standards	From supermarket shelves (2 and 3-piece cans)	10			Supermarket
	National Steel cans: 8.25 mil	20	20	15	National Steel
Unbeaded Steel	Manufacturer's Code:				
	DR8 Tempers:				
	6.6 mil 1122	10	40	20	Wierton Steel
	7.15 mil 1142	10	40	20	
	7.7 mil 1133	10	40	10	
	8.25 mil 9121	10	40	10	
	9.35 mil 1147	10	40	10	
	CAT4 Tempers:				
	8.25 mil 075224	10	40	10	
	8.8 mil 8852	10	40	10	
	9.9 mil 9448	10	40	10	
Aluminum Cans (unbeaded)	Coke/Sprite type	10	10	15	Supermarket
Note: 206 Radius	7-Up type	10	10	15	

double reduced. The DR8 temper is a stronger steel, useful for making thin cans. The thicknesses varied from 60 lb base box (6.6 mil) to 90 1 lb base box (9.9 mil), also common thicknesses for food cans.

For each can variable fifty cans were pressurized to varying degrees before load resistance testing. Ten cans were sealed at atmospheric pressure, ten pressurized to 6 psig, ten to 13 psig, ten to 20 psig, and ten to 26 psig. Ten cans were sealed at atmospheric pressure and tested for panel resistance. In two cases, twenty cans were given the panel resistance test, but there was no further increase in accuracy.

The unbeaded, two-piece aluminum cans with ends necked in were taken directly off of supermarket shelves for testing. Two types (Coca-cola and 7-up) were tested representing two slightly different geometries. For the panel resistance test, 15 cans of each type were emptied and sealed for testing. Ten aluminum cans of each type were tested for load resistance in their pressurized (40–45 psi) condition, and ten cans of each type were emptied for load resistance testing at atmospheric pressure.

Testing Methods

Load resistance was determined using a Universal testing machine. The cans were placed upright on the loading platform and a gradual compression was noted by the slow increase in load measured by the gauge needle. The maximum load withstood by the can before failure was the load resistance. After failure the needle would drop, especially when the material in the can yielded. However, buckling was also observed, and in some cases a single buckle would occur which preceded more general buckling by as much as 500 lb. The needle on the load gauge would then pause or drop slightly before continuing to rise. At general buckling, the load would drop considerably and continued compression would result in permanent deformation. In the case of buckling, load resistance was considered to be the load at which general buckling occured.

Panel resistance was determined by pressurizing the chamber of individual can retorts with compressed air. Panel resistance was read by a pressure gauge attached to the chamber. The pressure in the chamber was allowed to increase slowly until failure was indicated by the sharp decrease in the pressure gauge reading when the the can buckled; also failure could usually be heard. A more sensitive method of testing panel resistance was required for the aluminum cans, which buckle below 3 psi. A glass jar, large enough to enclose an aluminum can, was pressurized with a bicycle pump. A water manometer was used to measure the pressure.

Panel resistance is a pressure valve, and it is the pressure difference across the can which matters. That is, if an unpressurized can fails at 15 psig, then the same can pressurized to 5 psi would be expected to fail at 5 +15, or 20 psig.

Therefore, the test cans did not require pressurization for the panel resistance test. A single battery of tests, done on cans sealed at atmospheric pressure, would provide the panel resistance at any internal pressure.

Pressurizing Procedure

An open can was placed on a digital balance with a resolution of 0.001g and tared. A piece of dry ice at least 0.1g larger than required was placed in the can and allowed to evaporate. As it evaporated, the weight measured by the balance would slowly diminish. When the target weight was reached, the can was lidded and seamed immediately. Further evaporation of the dry ice created the internal pressure.

Three tests were run to measure the reliability of this pressurizing procedure. A number of cans were pressurized with three different weights of dry ice, and their pressures measured after the ice had evaporated (2–5 h). A bottle headspace gas sampler was used to test pressure.

In practice, it was difficult to predict the pressure which would be attained by a particular amount of dry ice, even though the dry ice procedure was found to be quite consistent. Note also that testing for pressure was done at the expense of the pressure in the can. For this reason, in all the load resistance tests eleven cans would be given the same quantity of dry ice. Ten would be tested for load resistance, and the eleventh tested for pressure alone, and the pressure found in this can would be the assumed pressure in the other ten.

For the unbeaded steel cans, there were actually eighty-eight cans which received the same amount of dry ice. Although these cans varied in thickness, their enclosed volume was the same, so the pressures developed in them should be the same. Eighty of the cans would be tested for load resistance, and eight tested for pressure. Also, it often happened that failure of a can occured without a visible indication of deformation. Yielding would be noticed first from a fall in the load needle, and second by an appearance of deformation. Even buckling, in many cases, was elastic, so that removal of the load returned the can to its original condition. For this reason, cans which did not show significant deformation after the load resistance test were tested for pressure. In nearly every case, they agreed generally with the results obtained from the cans which had not been through the load resistance test.

Aluminum cans were tested for load resistance with the pressure caused by their contents, and were not pressurized independently. This pressure was found to be very consistent.

RESULTS AND DISCUSSION

Pressurizing Procedure

Table 2 presents the results of the three tests which were run to measure the consistency of the dry ice procedure in creating pressure. For pressurized cans to be tested for load resistance it seems unlikely that a 2-3 psi difference between cans would significantly affect results. Therefore, for the purposes of this study, the procedure was assumed precise enough, even at 25 psig. The pressure variations may largely be due to the pressure tester itself. The pressure reading seemed to vary slightly (1-2 psig) with the speed with which the plunger punctured the can lids.

TABLE 2.
PRESSURES IN CANS PRESSURIZED BY THE DRY ICE PROCEDURE

	Test Number		
	1	2	3
Amount of dry ice/can	0.503g	1.02g	2.071g
Number of Cans	10	30	20
Ave. Pressure	5.3 psig	13.5 psig	25.15 psig
Standard Deviation	0.42 psig	0.72 psig	1.11 paig
Range	5-6 psig	12-14.5 psig	23-27 psig

Pressurization of three-piece steel cans above 20 psi bulged the ends noticeably. At 40 psig, the ends began deforming (end buckling). Because of this, these cans were not pressurized above 30 psig for the load resistance tests.

Failure Modes

The cans tested for load resistance failed either by yielding or buckling, or with some combination of the two. All of the panel resistance tests ended in buckling failure.

Yielding under compression was observed as a slow deformation of the metal in the sidewall. It was silent and gradual; once the sidewall had bent at the load resistance, a reduced load could continue the deformation. Yielding of cans in load resistance was so subtle that the first sign of yielding was a gradual leveling, then drop in the load gauge, Further compression was necessary before the deformation became visible.

Buckling, in contrast, was rapid, loud and very visible. Buckling is a geometrical failure, not a material one. It occurs when the can, as a unit, changes its shape instantaneously to reduce its overall strain energy. The cylindrical geometry of the can is shed for another one. If the can buckles under compression, the buckles appear as a pattern of diamond shaped dents in the sidewall. If under pressure, the cylinder may look like it is trying to assume a square or pentagonal shape. Although buckling can occur without material failure, yielding usually occurs in the bukled geometery. When it does, buckling under a constant load will lead to permanent deformation.

Beaded Steel Cans

Seven of the cans taken from supermarket shelves were three piece cans, and their average load resistance was 940 lb. Two of the cans were two piece cans with a 680 lb average load resistance. One can was three piece, but had a dent in the sidewall before testing. This can tested below 600 lb. The average load resistance for all these cans was 850 lb. From this limited test it appears that three-piece cans have a higher load resistance than two-piece cans. This is probably due to the geometry of the two-piece can, which has a shoulder due to forming which would not be very supportive of the axial compression load. The low value for the dented can is due to the concentration of stress that occurs around the dented area.

Forty National Steel cans, at four internal pressures were tested. Pressure actually did not make a great difference for these beaded cans, although there was a 10% increase in strength. The average load resistance was 1050 lb for unpressurized cans. These results are included in Fig. 1 and 2.

Failure in compression for these beaded cans was by yielding, which usually occured at the outside bead on the sidewall forming a six sided pattern. See Fig. 3a. This failure was expected, because the beading for an axial load serves only to concentrate stresses in the sidewall.

All the steel cans tested in this study gave a curious 'false yielding' during the load resistance test. The 'false yielding' was a short pause or brief downward movement in the load needle, after which the needle would continue its gradual increase to the actual failure. This occurred with fair consistancy at about 700 lb and again at 800 lb of load. Sometimes only one pause was noted. The cause may be a yielding of the sealant in the end seams of the cans.

The results from fifteen tests of panel resistance for the National Steel cans gave an average panel resistance of 43 psig, with very little variation. Failure was by loud buckling, with very large deformation as shown in Fig. 3b.

The results from our testing of beaded cans provide a basis for the acceptable strengths of steel food cans in this size class. The 303 × 406 can had a load resistance of about 900 lb, and a panel resistance of about 40 psig. These approximate strength values can be used as a standard when comparing the options that pressurization makes possible for food cans.
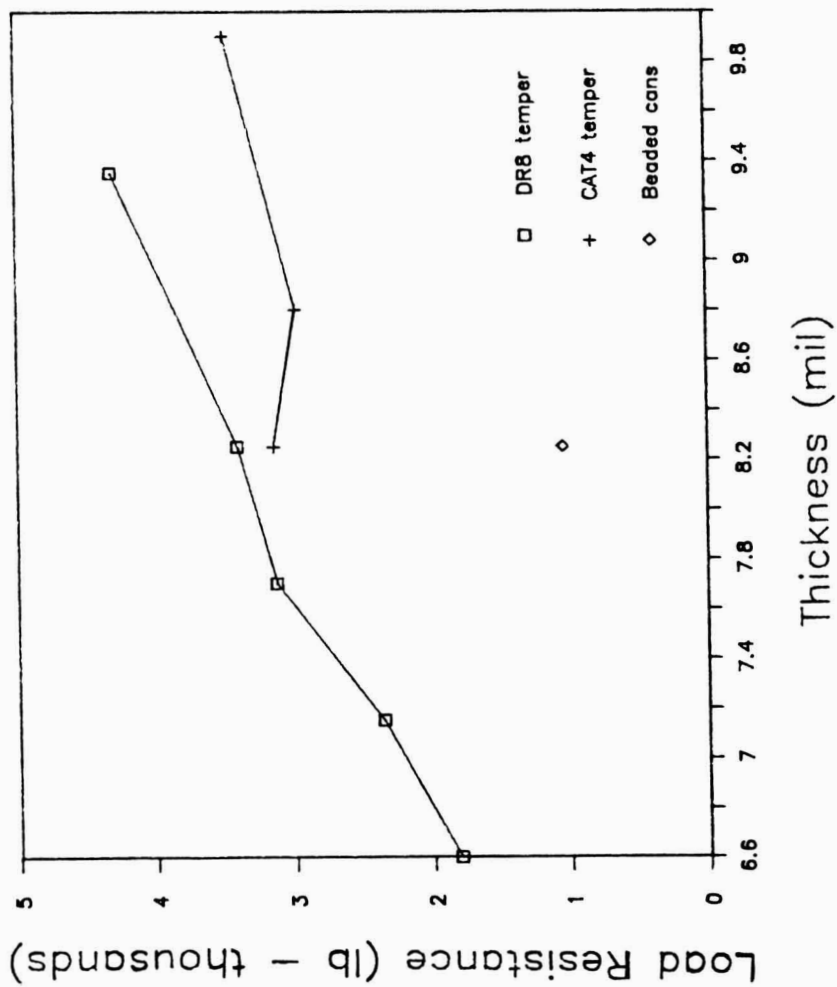
FIG. 1. LOAD RESISTANCE VS THICKNESS
FOR UNPRESSURIZED UNBEADED STEEL CANS
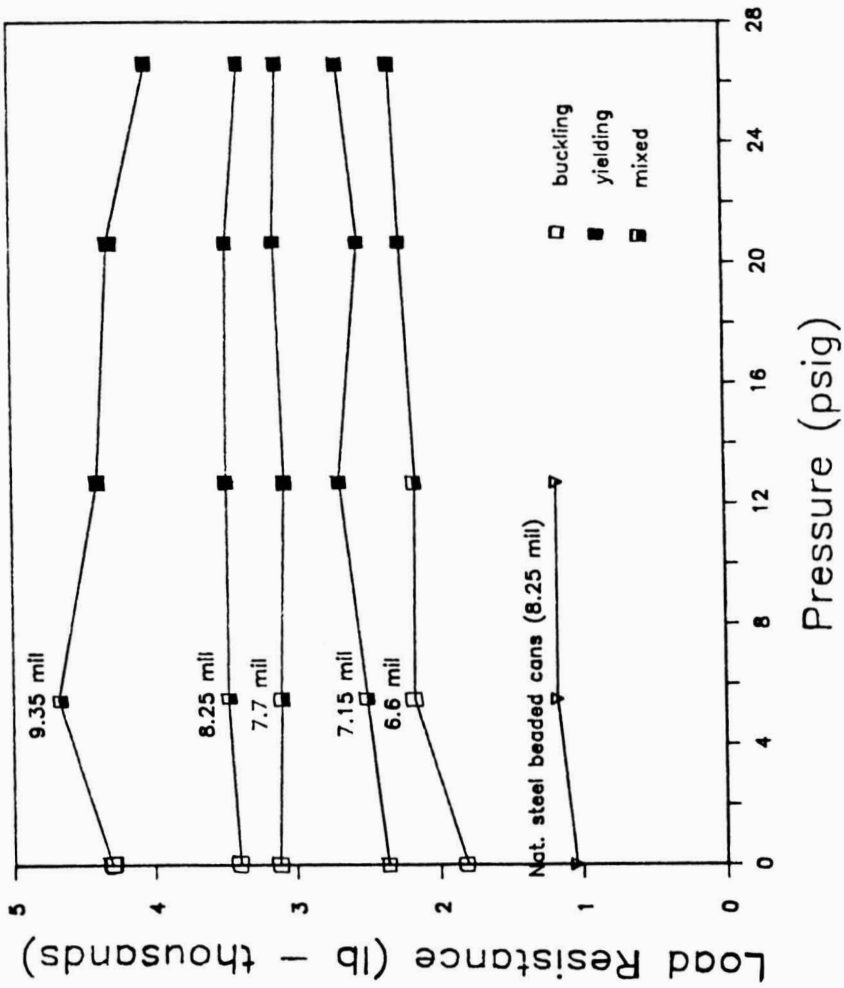
FIG. 2. LOAD RESISTANCE VS PRESSURE
FOR DR8 UNBEADED STEEL CANS
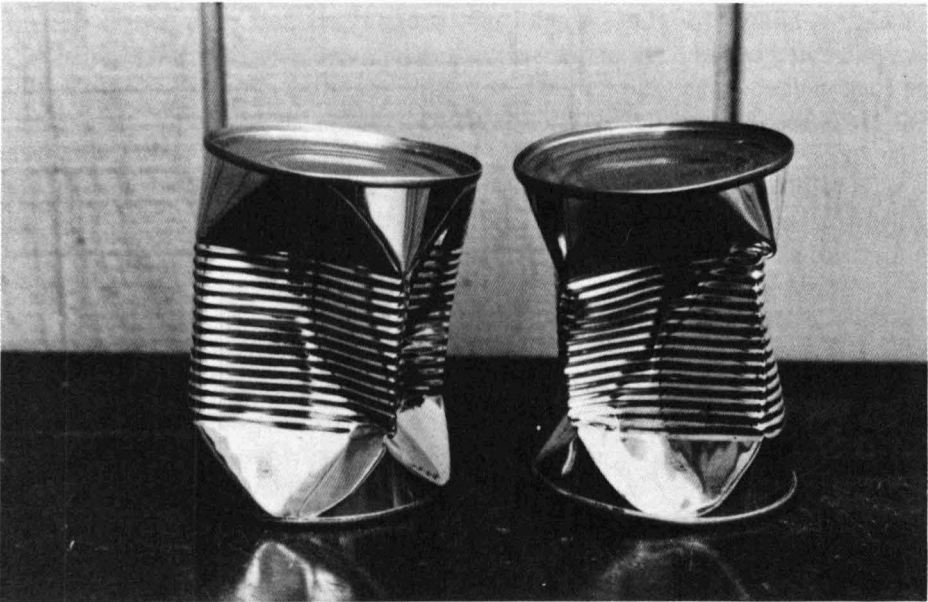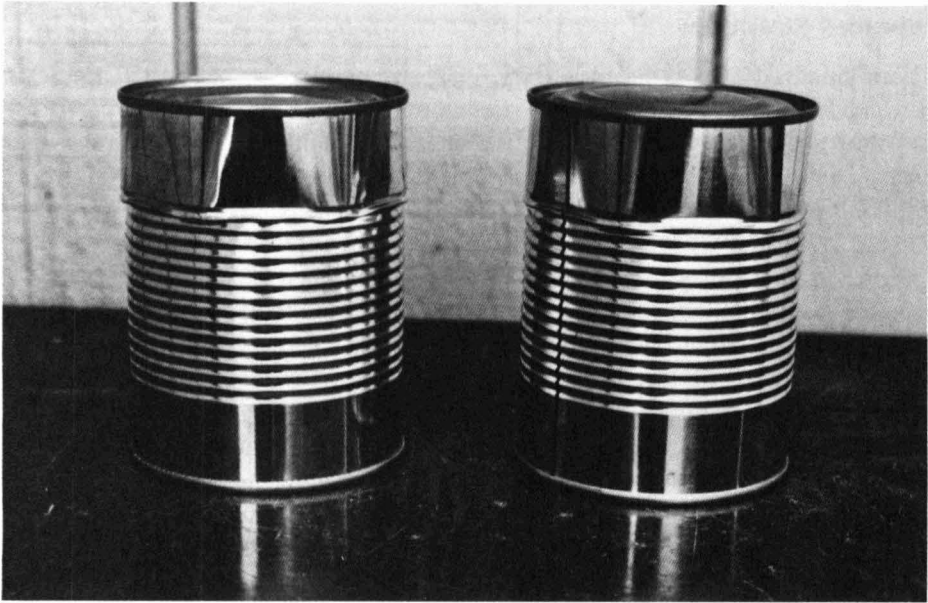
FIG. 3. BEADED STEEL CANS
a) Load Resistance Failure
b) Panel Resistance Failure

Unbeaded Steel Cans

Four hundred load resistance tests, and one hundred panel resistance tests were made on unbeaded steel cans. For unpressurized cans tested in compression the two tempers developed different kind of failures, and different load resistance trends. Figure 1 shows that CAT4 cans failed about 500-1000 lb short of the DR8 cans. The DR8 temper is the stronger one. Note that beading lowers the load resistance by over 2000 lb for the 8.3 mil cans.

Figure 1 also shows the effect of thickness on load resistance. For the DR8 cans, the average 9.4 mil can had a load resistance over twice that of the 6.6 mil. This expected trend did not entirely hold for the CAT4 cans. There the 8.8 mil cans actually had a lower average load resistance than the 8.3 mil. This was suspicious; can variables were examined for thickness and yield strength. It was found that despite the temper designation, the yield strength of the 8.8 cans was significantly lower than the 8.3 cans.

For these unpressurized cans, it was found in compressive failure that, with no exceptions, the DR8 cans buckled while the CAT4 cans yielded. Can temper is not an important variable in buckling failures. Therefore, if all the cans had buckled, there would only be one line in Fig. 1. The CAT4 cans yielded below the load at which they might have buckled.

Yielding failure for these steel cans, pressurized and unpressurized, was always located at the edge of the sidewall of the can, near the end seam. Only one edge yielded on any one can. There was no preference for which edge would yield first, the upper or lower end, as the can sat on the testing machine.

For the DR8 cans, the buckles were large, diamond shaped, and in a pattern along the sidewall. The thinner cans seemed to have a larger deformation, and a louder snap to the buckle than the thicker variables. Buckling and yielding failures are shown in Fig. 4a.

Pressurized cans gave the results shown in Fig. 2 and 5. Both figures show that for all the unbeaded cans, pressure does not significantly affect load resistance.

There was a pattern for the DR8 cans that, although not statistically significant, deserves comment. It appears that, for steel cans, the thinner the sidewall, the greater a role pressure can play in achieving desireable load resistances.

The DR8 cans buckled at zero pressure, but as their internal pressure increased, they began to fail by yielding. Figure 2 shows the type of failure that predominated for each variable at different pressures. The thicker cans switched to yielding at a lower internal pressure than the thin cans. At 26 psi, all of these cans were yielding in failure. Figure 4a shows typical failure progressions for 5 cans at increasing pressure. Note the large buckles at zero pressure. At 20 psi and above, failure is entirely by yielding.
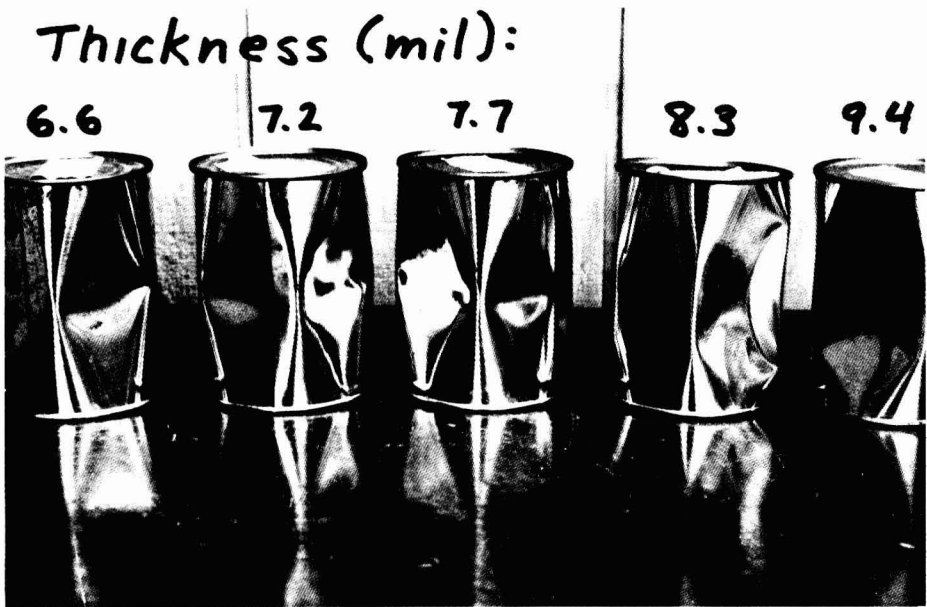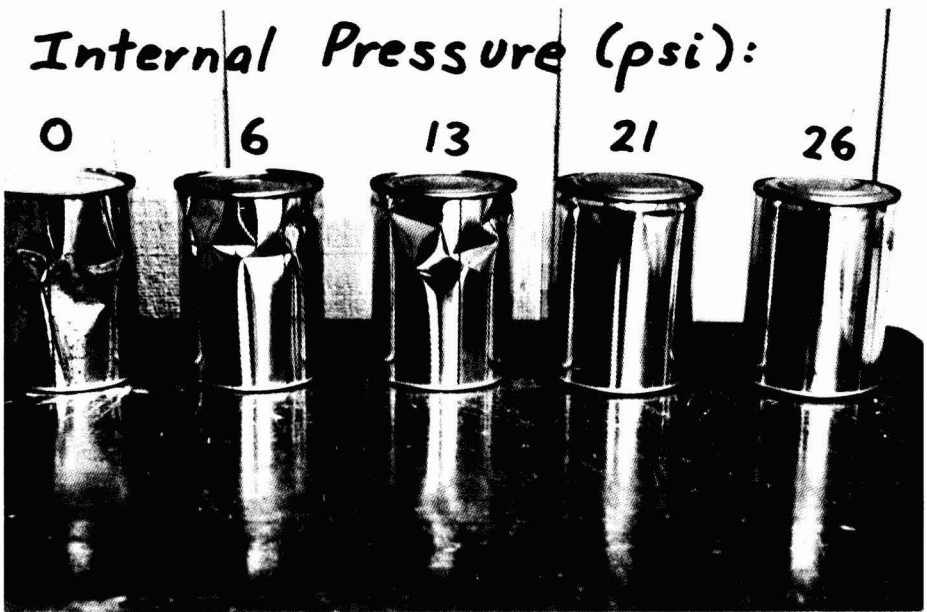
FIG. 4. UNBEADED STEEL CANS
a) Load Resistance Failure (DR8, 7.15 mil)
b) Panel Resistance Failure
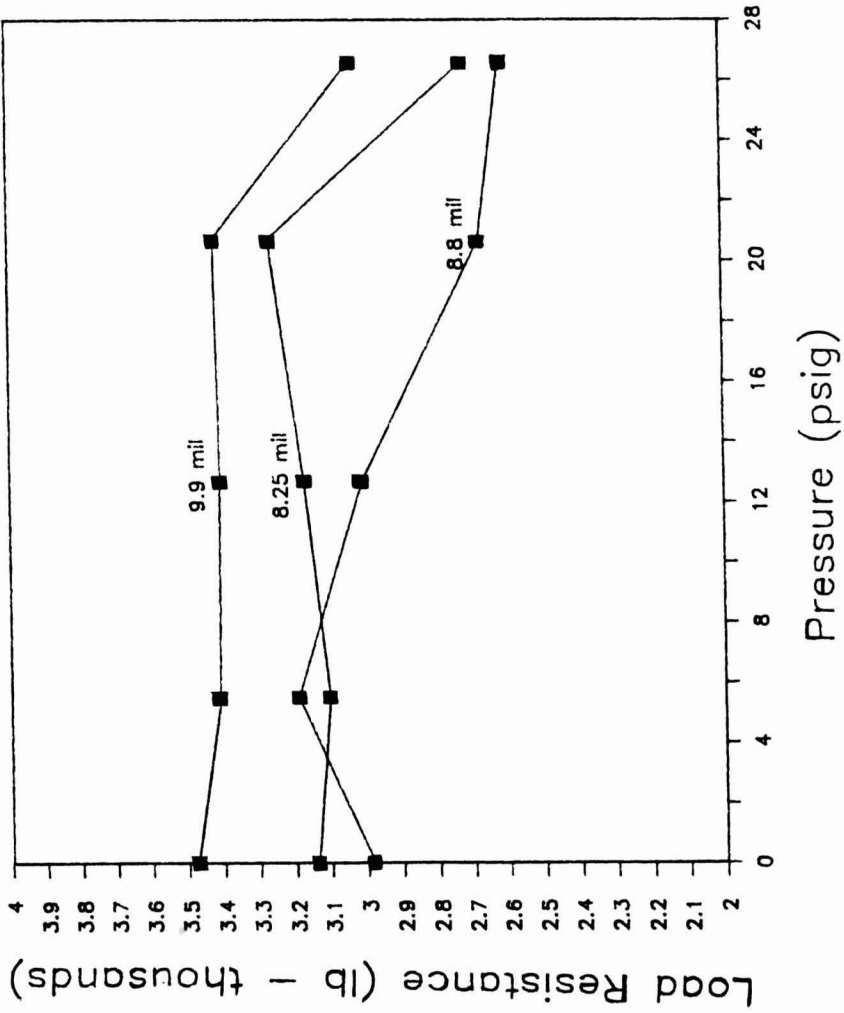
FIG. 5. LOAD RESISTANCE VS PRESSURE
FOR CAT4 UNBEADED STEEL CANS

The CAT4 cans showd no improvement in load resistance. Actually, there was a 13% decrease in these cans under internal pressure. It is felt that this decrease may be caused by the outward bending of ends which occurred with pressurization. This bending may place extra stresses on the sidewall near the edges which, in conjunction with the load stresses, caused the yielding at a lower load.

Panel resistance test results for the unbeaded steel cans were highly reproduceable. Typically, the results from ten determinations run on a single can variable would differ by less than one psi. All of the panel tests were done on unpressurized cans, and the results along with the results obtained for the beaded steel cans are presented in Fig. 6.

Comparing Fig. 6 with Fig. 1 one can see that can temper did not have the effect in paneling that it had in compression. For paneling tests all the cans buckled and for true buckling failure temper is not a factor. The type of buckling was typically a regular 5 sided pattern, as shown in Fig. 4b.

Figure 6 shows clearly the great influence of beading in improving panel resistance. The panel resistance of a 8.3 mil can be doubled by beading. Pressure also has a great influence; the same effect can be gained by pressurizing the can to 20 psig. In fact, pressure opens options not available to beading. An 8.3 mil thickness could be reduced 20% to 6.6 mil and, with 30 psig pressure, the panel resistance would be unaffected. Thus, the greatest potential from internal pressure for improving can strength is through its effect on panel resistance.

Aluminum Cans

Although the two can types tested differed in their geometry, the results were similar for both cans. Unlike the steel cans, pressure in aluminum cans has a very significant effect. The load resistances in both can types were doubled from 300 lb to 600 lb by pressurizing cans to 40 psig. Like the DR8 steel cans, there was a change in failure mode from buckling to yielding when the cans were pressurized.

Buckling failures at zero pressure were large deformation, loud, snap buckles. Yielding failure at 43 psig was, for both can types, at the edge of the sidewall at the upper shoulder. These cans are drawn so the thickness of the can is less at the upper shoulder than at the lower shoulder, which would explain the preference for failure at the upper shoulder.

Both aluminum cans had panel resistances of about 1.7 psi. The failure under external pressure was usually a four-sided even buckling. The aluminum cans, therefore, require all of their 43 psig of internal pressure to obtain a panel resistance of 45 psig when filled.

The beaded steel cans also had a panel resistance of about 43 psig in this study, so supermarket aluminum steel cans have roughly the same panel resistance. Yet panelled steel cans can be found in many supermarkets, while panelled
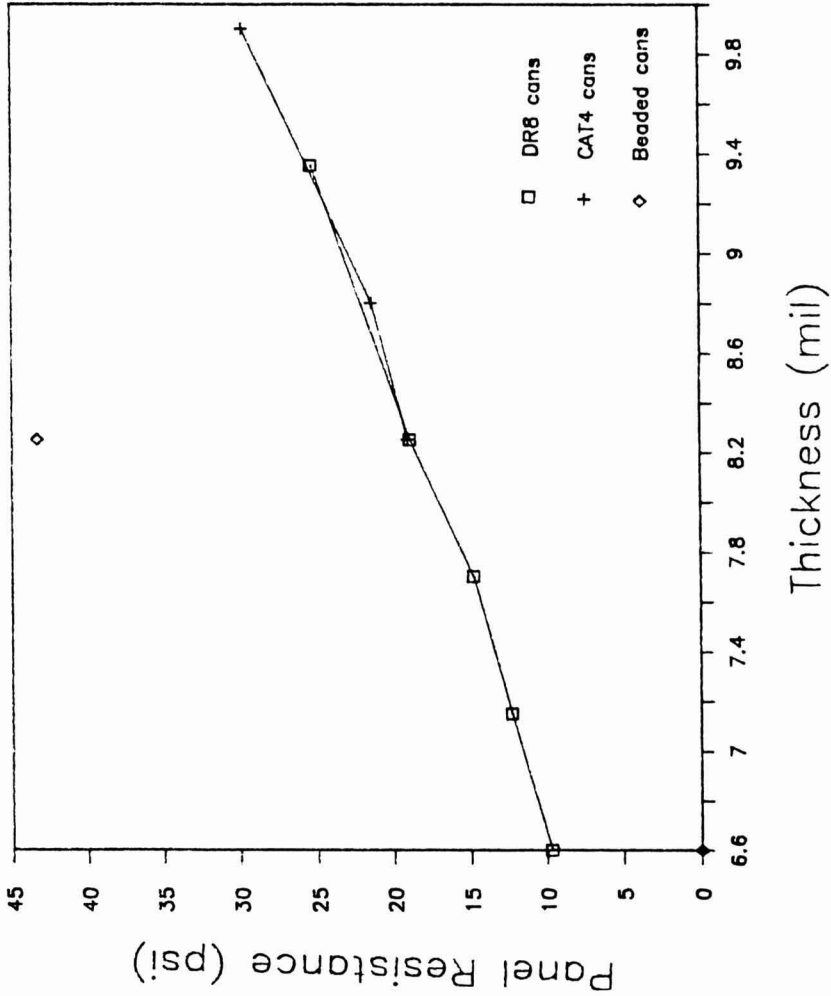
FIG. 6. PANEL RESISTANCE VS THICKNESS
FOR UNBEADED STEEL CANS

aluminum cans are much more difficult to find. This illustrates a problem with the panel resistance test as defined in this study; that two cans which test the same panel resistance may really have different panelling incidents. Steel cans deform permanently when given a sufficient concentrated load, but pressurized aluminum cans, thanks to their flexibility, deform only as long as the load is applied. It is probably more correct to say that the aluminum cans have a very large panel resistance pressure, because no pressure can leave a permanent panel mark on the can.

CONCLUSIONS

From tests on beaded steel cans, it appears that current practice in the canned food industry is to use 303×406 cans with approximately a 40 psi panel resistance and a 900 lb load resistance.

From tests on unbeaded steel cans, loss of beading does two things. First, it about triples the load resistance. Second, it about halves the panel resistance. This loss of panel resistance is significant to food canners trying to avoid panelled cans at the supermarket.

Tests with pressurized cans show that pressure could be used to supplement panel resistance without detrimentally affecting its load resistance. Pressure could also lead to the use of thinner can material.

With aluminum cans, much thinner and weaker than steel cans, pressure is required both for adequate load and panel resistance. With pressure, aluminum cans have a strength close to beaded steel cans: 43 psig panel resistance and 670 lb load resistance.

ACKNOWLEDGMENT

REFERENCES

ANON. 1981a. Tin-free steel cans move forward to lower food-can materials costs. Food Eng. *53*(12), 136.

ANON. 1981b. Foods demand for packaging. Food Eng. *53*(10), 64.

ANON. 1982. Cans fight back. IEFP show report. Food Eng. *54*(4), 93.

BREWBAKER, P.L. 1986. Strength Characteristics of Pressurized Cans, Un-published M.S. Thesis, University of California, Davis.

FRYE, C.A. 1984. Private communication. Reynolds Metals Co. Can Division. Richmond, VA.

KNILL, B.J. 1985. Coke tests 12-ounce PET soft drink can. Food and Drug Packaging *49*(12), 1.

LEONARD, E.A. 1980. *Packaging Economics*. Books for Industry, New York.

MCKERNAN, B.J. 1983. Developments in rigid metal containers for food. Food Technol. *37*, 134.

CONCENTRATION OF ORANGE JUICE
BY REVERSE OSMOSIS

BENJAMIN G. MEDINA and ALBERT GARCIA III

Department of Agricultural Engineering
Texas A&M University
College Station, TX 77843-2117

ABSTRACT

Orange juice was concentrated by RO up to 50% hydraulic recovery with a polyamide membrane. Permeate fluxes and solute recoveries were determined at transmembrane pressures of 6.21 and 4.14 MPa. Pectinase treatment was required to prevent fouling and to allow Cleaning in Place procedures. Enzymatic treatment did not affect permeate flux or solute recoveries. Overall recovery of sugars, organic acids, and flavor-volatile components was approximately 93%.

INTRODUCTION

Oranges are one of the largest fruit crops in the United States. The cultivation of orange trees takes place almost entirely in Florida, California, Texas and Arizona. The 1985–86 national harvest season yielded 7.5 million metric tons (T.A.S.S. 1987). Approximately 82% of this crop was processed and marketed as frozen concentrated orange juice. The processing plants are usually located near the production fields and involve a series of energy intensive operations including evaporation and quick freezing.

The established industrial practice for processing orange juice uses vacuum evaporators to concentrate the de-pulped juice to 62 °Brix which is then quick-frozen at −20°C for storage. The concentrate is later diluted with freshly squeezed juice, to 42 or 45 °Brix for retail distribution. The dilution is performed with fresh juices to return some of the natural flavors, and to offset the effect of heat on the overall quality of the juice.

Many of the compounds associated with fresh orange juice flavor are lost during multistage evaporation due to thermal exposure. Most of the citrus essences are volatilized in the first effect of the evaporator (Johnson and Vora 1983) while in the later stages other compounds are destroyed or converted to other nondesirable constituents such as furfurals (Nagy and Randall 1973). These detrimental effects of heat upon orange juice can only be avoided by utilizing concentration processes that are based on principles other than the evaporation

of water. The two most promising alternatives are freeze concentration and membrane concentration.

Concentration of liquid food products by membrane processes has been widely explored after the discovery of asymmetric membranes by Loeb and Sourirajan in 1960. In these processes, the retention of flavor compounds is a major factor regarding the quality of the final product (Merson *et al.* 1980). Ultrafiltration (UF) of fruit juices has generally not been recommended due to a low retention of essential flavoring compounds. Reverse osmosis (RO) has been proposed as a better alternative to UF due to the virtual rejection of almost all compounds of interest (Morgan *et al.* 1965; Yu *et al.* 1986).

The choice of membrane type is one of the major determining factors when assessing RO performance. Polyamide membranes have greater retention of flavor compounds and sugars but lower fluxes than cellulose acetate membranes (Sheu and Wiley 1983). It was decided by the authors that flavor and sugar retention were the more important consideration. Polyamide membranes are also known to have a longer useful life than cellulose acetate. This factor is significant because the annual replacement costs for membranes can be as high as 10% of the total RO plant investment (Thijssen and Van Oyen 1977; Paulson *et al.* 1985). Polyamide membranes were chosen for study due to these favorable characteristics.

The advantages of RO over the current multistage vacuum evaporation process for juice processing are: low thermal damage to product quality, reduction in capital equipment costs, lower energy consumption and increases in aroma and flavor retention (Merson *et al.* 1980). Due to these advantages, membrane concentration techniques have been previously tested on a variety of juices, such as oranges, tomatoes, apples, pears, kiwi and passion fruits (Merson and Morgan 1968; Dale *et al.* 1982; Wilson and Burns 1983; Sheu and Wiley 1983; Papanicolau *et al.* 1984; Yu and Chiang 1986; Rao *et al.* 1987). Nevertheless, there is not conclusive information about replacing conventional evaporators by membrane systems while obtaining the same total solids content and flavor profile in the final product.

In spite of the high selectivity and solute retention capacity of RO membranes, the concentration of fruit juices by this process has a significant drawback. The high osmotic pressure of fruit juices precludes their concentration to the required level of total solids. Studies have shown that for cellulosic and noncellulosic membranes the most efficient flux and solute recovery is at concentrations lower than 30 °Brix (Thijssen and Van Oyen 1977; Sheu and Wiley 1984; Pepper *et al.* 1985). Given the current industrial practice of concentrating orange juice to at least 42 °Brix, membranes processes should be viewed as a first stage process with other technologies like freeze concentration or evaporation completing the concentration system.

The maximum concentration level attained by an RO process will be determined by the osmotic pressure of the juice and the economics of a diminishing flux with a fixed capital investment. Even though an RO process will be unable to provide complete concentration, it will be able to remove more than half of the water. Thus, as RO process could be used to increase the capacity of existing equipment while reducing thermal exposure. The combination of RO with flavor enhancing but more expensive concentration processes could prove to be a feasible alternative to evaporation.

This experiment was undertaken to assess the potential role and suitability of reverse osmosis as a concentration process for orange juice. The specific objectives of this project were to evaluate the overall performance of a composite polyamide spiral wound membrane module, the effect of pressure on permeate flux, the rejection and solute recovery of flavor components, sugars and acids, and the effect of pectinase treatment on flux.

MATERIALS AND METHODS

Preparation of Orange Juice

The experimental trials were done with pasteurized single strength orange juice supplied by Texas Citrus Exchange (Mission Texas) during the 1986–1987 harvest season. The 600 L batch was taken out of the processing line before the evaporators and passed through a tube pasteurizer at 85 °C for 45 s. One third of the batch was enzymatically treated. This treatment consisted of adding 400 ppm of a pecticnolytic enzyme preparation (Pectinol 80SB, Genecor, San Francisco, CA.) at 30 °C for 2 h and constant stirring. To stop the enzymatic action, the juice was pasteurized at 85 °C for 18 s.

Reverse Osmosis Equipment and Procedures

The RO system consisted of a spiral wound 192 MS02-P membrane with 1.28 m² of effective area, a 192T stainless steel pressure vessel, both made by Osmonics (Minnetonka, MN), a 3-cylinder piston pump (Hypro model 1812B, St. Paul, MN) and a pulsation dampener (Hypro model 3375-0010, St. Paul, MN). The triplicated experiments were conducted at 20 °C and at two transmembrane pressures of 4.140 a 6.210 MPa (Fig. 1). The concentrate was recirculated at 15 L/min and the permeate was accumulated and compared to the initial orange juice volume to determine hydraulic recovery. Samples of initial feed, concentrate and permeate were collected at recoveries of 0, 10, 20, 30, 40, and 50%, corresponding to weight concentration ratios (WCR) of 1, 1.11, 1.25, 1.43, 1.67, and 2.00. Permeate and concentrate flow rate, temperature, °Brix,
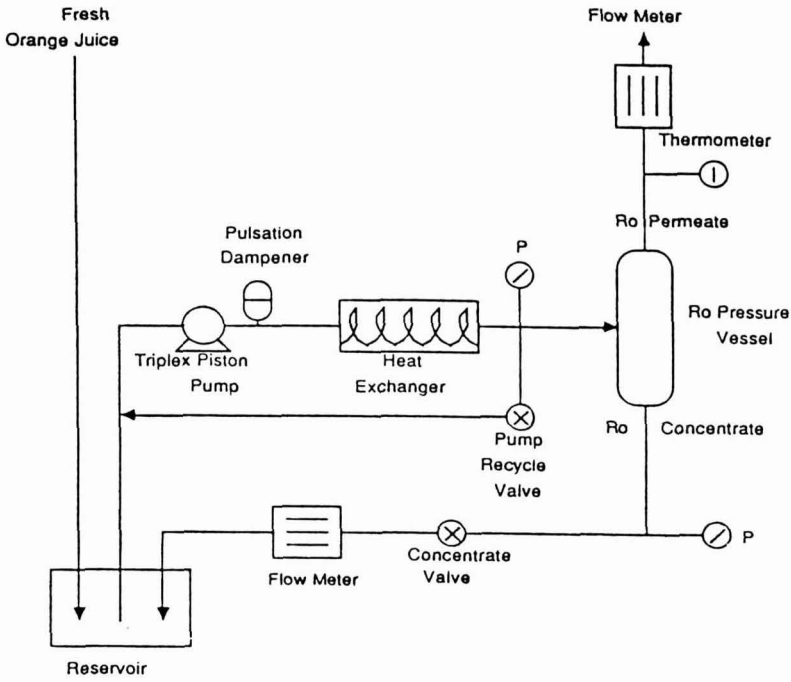
FIG. 1. RO SYSTEM SCHEMATIC

pH and elapsed time were recorded at collection time and samples were immediately frozen at $-18\,°C$ for subsequent analyses. The membrane was used as specified by the manufacturer for operational conditions, pressures, pH values and cleaning. Cleaning procedures were performed with the pressure control valve fully open and consisted of tap water rinsing for 10 min, use of a recirculating 0.1% NaOH solution or/and Ultrazyme detergent (Osmonics, Minnetonka, MN) both for 15 min, followed by water rinsing during 10 min.

The average processing capacity of the membrane was calculated by dividing the permeate volume at the end of each run by the average total time of each treatment. The solute recovery was calculated by dividing total solute mass present in the concentrate by the total solute mass present in the feed at 50% of hydraulic recovery. The rejection values for the membrane were calculated using the following formula, suggested by N.T.I.S. (1976).

$$\% \text{ Membrane Rejection} = \frac{\ln [C_f/C_c]}{\ln [1 - P_w]}$$

C_f = Initial Feed Concentration
C_c = Concentrate Concentration at a Specific Hydraulic Recovery
P_w = Hydraulic Recovery

Analytical Methods

The volatile flavor compounds were extracted from the samples using a modification of the method described by Braddock and Adams (1984). The gas chromatograph (GC) operational conditions were developed in our laboratory.

Ten mL samples of feed, concentrate or permeate were mixed with 3 mL of dichloromethane and agitated for 1 min; then they were centrifuged for 10 min at 4000 rpm. After centrifugation, 1.5 mL of the dichloromethane phase was dried over anhydrous sodium sulfate that was subsequently washed with 1 mL dichloromethane. A known amount of 2, 6-Dimethylphenol (Aldrich Chem. Co., Milwaukee, WI) was added to the extracts as internal standard. Previous to injecting, the extract was concentrated at room temperature to around 0.5 mL with nitrogen gas.

Gas chromatographic analyses were performed by injecting 0.5 μL samples, splitless mode, in a Tracor 560 GC System with flame ionization detector and connected to an IBM Instruments Model 9000 computer with IBM Chromatographic Applications Program (CAP) software for collection and quantitation of the peak areas. A 30 m SP-2330 glass capillary column (Supelco, Inc., Bellefonte, PA) was used as the stationary phase. Column temperature was programmed from 45 to 200 °C at 6 °C/min, initial and final hold were 5 and 10 min, respectively. Injection port temperature was set to 220 °C and the detector at 250 °C. The chemical identification of the peaks was done with a VG model 70, model focussing mass spectrophotometer with a DS 11/250J Datasystem and a Hewlett-Packard 5890 chromatograph. The capillary column and the chromatographic conditions were similar to the above described.

Organic acids were analyzed by an HPLC equipped with a differential refractometer detector. Samples for analysis were centrifuged at 6000 rpm for 10 min. The supernatant was diluted 1:10, and passed through a C18 Pre-Sep column (Fisher Sci. Co.). The detemination of citric and malic acid was performed as suggested by Ting and Ruoseff (1986) with a C18 column (Alltech, Deerfield, IL).

Glucose, fructose and sucrose were determined with a YSI Industrial Analyzer (YSI, Inc., Yellow Springs, OH). Feed OJ samples were diluted 1:2 and a 25 μL injection was made in duplicate for each specific sugar. Permeate samples were injected in the same amount with no dilution. The solute recovery percentage was calculated at 2.0 WCR or 50% hydraulic recovery using the following formula:

$$\% \text{ Solute Recovery} = \frac{\text{Solute Conc. Feed - 0.5} \times \text{Solute Conc. Permeate}}{\text{Solute Conc. Feed}} \times 100$$

Statistical analyses were performed using Statistical Analytical System software (SAS Institute Inc., Raleigh, NC). Experimental data were analyzed for statistical significance using analysis of variance (ANOVA) and Fischer's protected LSD test was utilized for muliple comparisons between means with a probability of error fixed at 5%.

RESULTS AND DISCUSSION

Permeate Flux and Processing Capacity

The choice of an operating temperature involved the consideration of factors that relate to product quality or process feasibility. The polyamide membrane used in these trials could be operated within a temperature range of 0 to 40 °C giving suitable flexibility for operation. The permeate flux of RO membranes typically increases as RO operational temperature increases thus favoring the choice of a high temperature. However, a gel mix, assumed to be mostly pectin and cellulose, heavily precipitated on the membranes surface at temperatures of 40 °C during our initial trials with orange juice concentration. Furthermore, previous RO trials with apple juice have shown that at 45 °C reduced volatile flavor compounds retention by 50% (Sheu and Wiley 1983). Since, fouling and flavor retention were the more important consideration, these trials were performed at 20 °C.

The applied hydrostatic pressure minus the osmotic pressure difference of the feed is the driving force in any RO system. Since the osmotic pressure is a function of solute concentration, flux will decrease as hydraulic recovery increases (Fig. 2).
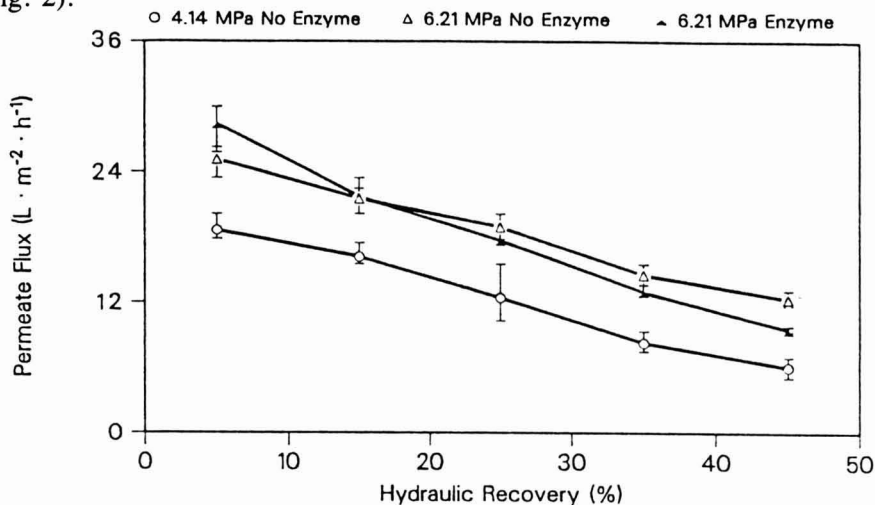

FIG. 2. PERMEATE FLUX AS A FUNCTION OF HYDRAULIC RECOVERY

The differences between the curves for enzyme-treated and untreated juice response at the higher pressure may be attributed to two factors (Fig. 2). The first factor was the prevention of pectin fouling layer formation (Watanabe *et al.* 1979). The second factor could have been due to an increase in osmotic pressure of the enzymatically treated juice caused by solubilization of pectin to oligogalacturonates (Baker and Bruemmer 1972). From 0 to 15% hydraulic recovery, the permeate flux of enzyme-treated juice was higher than the untreated juice at the same pressure due to reduction of the pectin layer. However, as the hydraulic recovery increased, the higher permeation rate attributed to elimination of the pectin layer was offset by the lower net pressure, a consequence of the higher osmotic pressure of the enzyme-treated juice. Overall the enzyme treatment at 2.0 WCR did not change the average processing capacity (Table 1).

TABLE 1.
AVERAGE PROCESSING CAPACITY AT 2.0 WCR

Triplicated Treatment	Average Processing capacity $[L \cdot m^{-2} \cdot h^{-1}]$
6.21 MPa No Enz	16.29 a
6.21 MPa Enz	15.63 a
4.14 MPa No Enz	10.44 b

a,b significantly different at 5%

The average processing capacity for the RO treatment is a measure of the membrane's performance and is used as an initial design parameter for Ro systems (Table 1). The suggested economically feasible processing capacity for RO systems depends mainly on product type and cost, module and membrane type, energy costs, and alternative processes (Paulson *et al.* 1985). However, apple juice is considered to be over 15.0 $L \cdot m^{-2} \cdot h^{-1}$ (Sheu and Wiley 1983). The average processing capacity for both treatments at 6.21 MPa were above the mentioned limit.

Retention of Some Flavor-Volatile Components

The volatile flavor components impart a fresh juice-like flavor to concentrated citrus products. The concentration of fresh citrus juice, in high temperature evaporators, virtually eliminates all of the volatile flavor components during the first 25% of the evaporation process (Johnson and Vora 1983). Therefore, volatile components are an essential consideration when evaluating RO as a prospective substitute concentration process.

The determination of flavor-volatile components was performed in all the treatments. The nonenzymatically treated samples indicated a considerable loss of these compounds probably due to entrapment in the pectin and cellulose fouling layer detected on the unwound membrane's surface. The small amount of insoluble carbohydrates, no more than 0.1% wet basis (Ting and Rouseff 1986), contained in 50 L of orange juice was sufficient to foul in the 1.28 m² of effective membrane area. It was therefore impossible to appropriately compare the effect of pressure on the flavor-volatiles of nonenzymatically treated juice. For the enzymatically treated trials the solute recovery was highly acceptable (Table 2) when compared to the total loss of volatile components during high temperature concentration process.

TABLE 2.
SOLUTE RECOVERY AND MEMBRANE REJECTION OF
VOLATILE FLAVOR COMPONENTS AT 2.0 WCR AT
6.21 MPa WITH ENZYME TREATMENT

Flavor Component	Solute (#) Recovery (%)	Membrane Rejection (%)
d-Limonene	89.0	83.1
Linalool	87.3	80.5
Ethyl Furoate	95.0	92.6
Sesqui terpene C15H24*	80.5	68.8
-Terpineol	92.1	88.1
Oxy-Compound*	92.5	88.7

* = specific isomer was unidentified
# = Pooled standard deviation 2.6 %

The GC chromatograms for the permeate extracts did not include the peaks detected in the concentrate or the feed juice in any of the experimental trials (Fig. 3). Therefore, the losses of terpenic compounds could be attributed to changes in the juice due to the mechanical effects of high-pressure pumping rather than to membrane permeation. This high degree of lability of these substances is further illustrated in that they have been shown to decrease more than 90% with short time pasteurization (Schreier et al. 1977). The peak appearing at about 8 min retention time is solvent contamination, chlorobenzene, and the peak height is a consequence of dichloromethane concentration after sample extraction.

Retention of Sugars

The 9.8 °Brix juice used for these trials was a 7.0% sugar solution containing 3.69% sucrose, 1.55% glucose, and 1.74% fructose. The retention of sugars in the concentration of fruit juices is important because of sweetness, sugar/acid
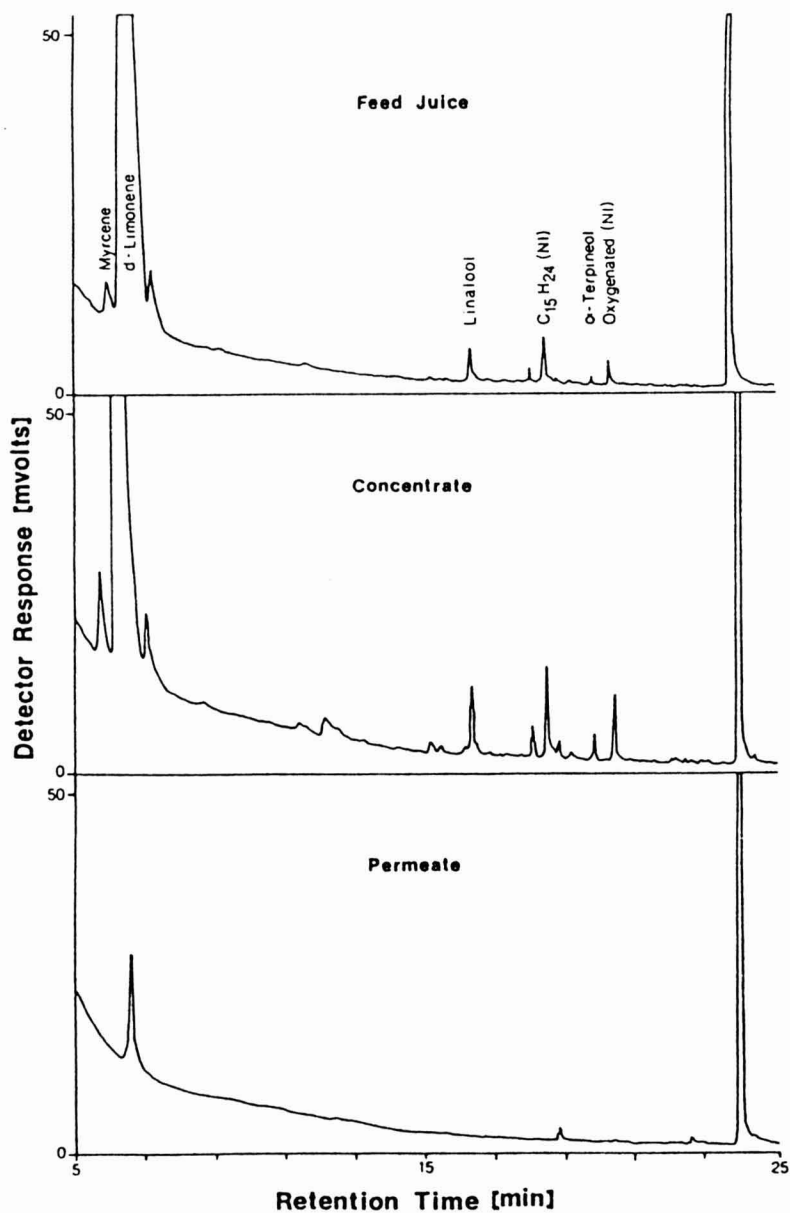
FIG. 3. GC CHROMATOGRAMS FOR VARIOUS FLAVOR COMPOUNDS

ratio, and their overall organoleptic contribution. In addition, the sugar content of the fruit is used by the processor to determine the amount of water to be removed before reaching the required concentration.

TABLE 3.
SOLUTE RECOVERY OF SUGARS AT 2.0 WCR

Triplicated	Sugar Recovery		
Treatment	Sucrose(%)	Glucose(%)	Fructose(%)
6.21 MPa No Enzyme	99.7	99.5	98.4
6.21 MPa Enzyme	99.3	99.2	98.1
4.14 MPa No Enzyme	99.4	99.3	98.3

data not significantly different at 5% level

The mean sugar recoveries were not statistically different for different pressures or enzymatic treatment. These sugar recoveries were similar to the values reported for noncellulosic membranes in apple juice concentration (Sheu and Wiley 1984; Pepper *et al.* 1985). These high sugar recoveries are important if RO is to be considered a viable concentration process option.

Retention of Organic Acids

Citric and malic acids are the main organic acids in citrus fruits and they represent from 50%, in very young fruits, to 90% in mature fruit of all present organic acids (Vandercook 1975). Besides being a legal indicator of maturity, these acids are important to recover because the acidity level is critical to consumer acceptance. Despite their different molecular size both acids have very similar recoveries (Table 4). As a result of the acid retention the pH values for feed and concentrated streams were different. The average pH values were 4.1 and 5.1 for the concentrate and permeate, respectively.

TABLE 4.
SOLUTE RECOVERY OF ORGANIC ACIDS AT 2.0 WCR

Treatment	Organic Acids Recovery	
	Malic(%)	Citric(%)
6.21 MPa No Enz	86.5	83.2
6.21 MPa Enz	88.3	84.6
4.14 MPa No Enz	84.4	84.9

data not significantly different at 5% level

Effect of Enzymatic Treatment

The enzymatic treatment did not significantly affect the permeate flux at 6.21 MPa. However, it was effective in preventing the formation of the pectin fouling layer visually observed in the trials without enzymatic treatment. With enzymatic treatment the membrane needed only recirculation with a 0.05% NaOH solution to be cleaned enough to recover its initial flux. After three consecutive trials, with only rinsing and 0.05% NaOH solution recirculation for 10 min at the end of each, the unwrapped membrane did not sow signs of pectin and cellulose layer build-up.

Three hours after the RO process, the enzyme-treated juice showed some detectable settling that increased with time. The problem of cloud stabilization can be solved by selecting an enzyme formulation intended for this purpose or by regulating enzyme concentration. The most effective pectinases for cloud stabilization are those with high polygalacturonase and low polymethylgalacturonase activity (Baker and Bruemmer 1972).

Performance of the Membrane

The recirculation flow rate (15 L/min) was the maximum rated for the membrane cartridge used. The highest rate was chosen to minimize concentration polarization and pectin and cellulose fouling layer formation. After four runs, with a new membrane, the initial permeate flux decreased more than 50% of its original rate if only the described cleaning regimen was used. To solve this problem the membrane had to be unwrapped and cleaned by hand, with a sponge and water. Then, the membrane's initial flux was recovered, the collected data was discarded, and the hand cleaning procedure was performed, after each RO process, for trials without enzymatic treatment.

Trying to eliminate the membrane's unwrapping step, several cleaning in place procedures were tested. They included water rinsing and recirculation up to 20 min of 0.5% NaOH, 0.5% phosphoric acid, and 1% Ultraenzyme solutions, individually or in combined steps, at 30–35 °C. The cleaning procedures were unable to restore the membrane's permeate flux to the level of the previous trials. Thus, the addition of pectinases should be viewed as an important pretreatment in the RO process.

The solute and membrane rejection were calculated as mean overall recovery for volatile-flavor components, sugars and organic acids (Fig. 4). The recovery of flavor components determined by GC was higher than expected. Almost 70% of the orange juice dry matter is sugars, therefore it is important that sugar recovery be high to allow the process to be scaled up. Sugar recovery was higher than acid recovery, therefore the Brix/Acid ratio will increase during the RO process, thus improving one of the quality indicators.
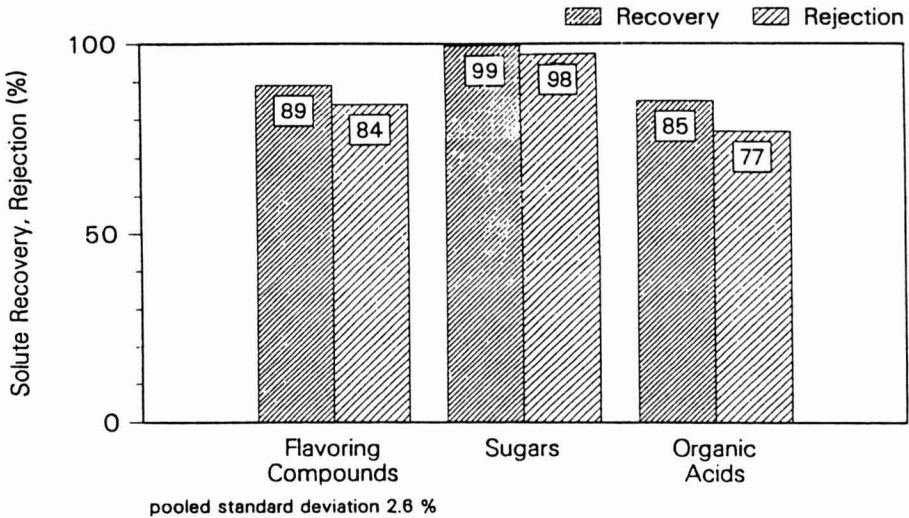
FIG. 4. OVERALL SOLUTE RECOVERY AND REJECTION FOR VARIOUS COMPOUNDS

CONCLUSIONS

The processing capacity for 6.21 MPa and 50% hydraulic recovery was 18% above the economically feasible limit for RO process established for apple juice by Sheu and Wiley (1983). The overall solute recovery for flavor-volatile components, acids and sugars were considered acceptable. Due to the unequal membrane rejection of sugars and organic acids the °Brix/acid ratio increased making sweetness more perceptible. The controlled solubilization of pectin by addition of pectinolytic enzymes was important to prevent membrane fouling and to allow cleaning in place procedures.

Reverse osmosis concentration could be established as the first stage of a process to produce high quality frozen concentrates. The RO process at a 50% hydraulic recovery can eliminate at least 63% of the water that is removed from fresh orange juice in conventional high-temperature concentration. The subsequent water removal could be accomplished by using freeze concentration or vacuum evaporation to obtain a high quality frozen concentrated orange juice. However, more research needs to be done to optimize the enzymatic treatment of the juice and to test other membranes that could further improve organic acids recovery.

REFERENCES

BAKER, R.A. and BRUEMMER, J.H. 1972. Pectinase stabilization of orange juice cloud. J. Agr. Food Chem. *20*(6), 1169.

BRADDOCK, R.J. and ADAMS, J.P. 1984. Recovery of citrus oils by ultrafiltration and reverse osmosis. Food Technol. *38*(12), 109–111.

DALE, M.C., OKOS, M.R. and NELSON, P. 1982. Concentration of tomato products: analysis of energy savings process alternatives. J. Food Sci. *47*, 704.

JOHNSON, J.D. and VORA, J.D. 1983. Natural citrus essences. Food Technol. *37*(12), 82–83, 97.

LOEB, S. and SOURIRAJAN, S. 1960. Sea water demineralization by means of a semipermeable membrane. UCLA Water Resources Center Report WRCC-34, Los Angeles, CA.

MERSON, R.L., PAREDES, G. and HOSAKA, D.B. 1980. Concentrating fruit juices by reverse osmosis. In *Ultrafiltration Membranes and Applications.* p. 405. Plenum Publishing, New York.

MERSON, R.L., and MORGAN, A.I. 1968. Juice concentrations by reverse osmosis. Food Technol. *22*(5), 97–100.

MORGAN, A.I., LOWE, E., MERSON, R.L. and DURKEE, E.L. 1965. Reverse osmosis. Food Technol. *19*, 1790–1792.

NAGY, S. and RANDALL, V. 1973. Use of furfural content as an index of storage temperature abuse in commercially processed orange juice. J. Agric. Food Chem. *21*, 272.

N.T.I.S. 1979. Reverse osmosis technical manual. National Technical Information Service. #B80-186950.

PAPANICOLAU, D., KATSABOXAKIS, K. and CODOUNIS, M. 1984. Comparison of the qualitative characteristics of concentrated orange juice by reverse osmosis and vacuum evaporation during frozen storage. p. 211. Reveu Generale du Froid, Avril.

PAULSON, D.J., WILSON, R.L. and SPATZ, D.D. 1985. Reverse osmosis and ultrafiltration applied to the processing of fruit juices. In *Reverse Osmosis and Ultrafiltration.* p. 325. ACS Symp. Ser. 281, Washington, DC.

PEPPER, D., ORCHARD, A.C.J. and MERRY, A.J. 1985. Concentration of tomato juice and other fruit juices by reverse osmosis. Desalination *53*, 157–166.

RAO, M.A., ACREE, T.E., COOLEY, H.J. and ENNIS, R.W. 1987. Clarification of apple juice by hollow fiber ultrafiltration: Fluxes and retention of odor actives volatiles. J. Food Sci. *52*, 375.

SCHREIER, P., DRAWERT, F., JUNKER, A. and MICK, W. 1977. The quantitative composition of natural and technologically changed aromas of plants. II Aroma compounds in oranges and their changes during juice processing. Z. Lebensm. Onters. Forsch. 164, 188–193.

SHEU, M.J. and WILEY, R.C. 1983. Preconcentration of apple juice by reverse osmosis. J. Food Sci. 48, 422.

SHEU, M.J. and WILEY, R.C. 1984. Influence of reverse osmosis in sugar retention in apple juice concentration. J. Food Sci. 49, 304.

T.A.S.S. 1987. Texas Citrus, Texas Agricultural Statistical Service. June.

THIJSSEN, H.A.C. and VAN OYEN, N.S.M. 1977. Analysis and economic evlauation of concentration alternatives for liquid foods. Quality aspects and cost of concentration. J. Food Process Eng. 1, 215.

TING, S.V. and ROUSEFF, R.L. 1986. *Citrus Fruits and Their Products.* pp. 20 and 93. Marcel Dekker, New York.

VANDERCOOK, C.E. 1975. Organic acids. In *Citrus Science and Technology.* Vol. 1. p. 210. Van Nostrand Reinhold/AVI, New York.

WATANABE, A., OHTA, Y., KIMURA, S. and UMEDA, K. 1979. Fouling material on reverse osmosis membranes during concentration of mandarin orange juice. Nip. Shoku. Kagyo Gak. 26(6), 260.

WILSON, E.L. and BURNS, D.J.W. 1983. Kiwifruit juice processing using heat techniques and ultrafiltration. J. Food Sci. 48, 1101.

YU, Z.R. and CHIANG, B.G. 1986. Passion fruit concentration by ultrafiltration and evaporation. J. Food Sci. 51, 1501.

YU, Z.R., CHIANG, B.H. and HWANG, L.S. 1986. Retention of passion fruit juice compounds by ultrafiltration. J. Food Sci. 51, 841.

PUBLICATIONS IN
# FOOD SCIENCE AND NUTRITION

F
N
P

Journals

JOURNAL OF MUSCLE FOODS, N.G. Marriott and G.J. Flick
JOURNAL OF SENSORY STUDIES, M.C. Gacula, Jr.
JOURNAL OF FOOD SERVICE SYSTEMS, O.P. Snyder, Jr.
JOURNAL OF FOOD BIOCHEMISTRY, J.R. Whitaker, N.F. Haard and
    H. Swaisgood
JOURNAL OF FOOD PROCESS ENGINEERING, D.R. Heldman and R.P. Singh
JOURNAL OF FOOD PROCESSING AND PRESERVATION, D.B. Lund
JOURNAL OF FOOD QUALITY, R.L. Shewfelt
JOURNAL OF FOOD SAFETY, J.D. Rosen and T.J. Montville
JOURNAL OF TEXTURE STUDIES, M.C. Bourne and P. Sherman

Books

CONTROLLED/MODIFIED ATMOSPHERE/VACUUM PACKAGING OF
    FOODS, A.L. Brody
NUTRITIONAL STATUS ASSESSMENT OF THE INDIVIDUAL, G.E. Livingston
QUALITY ASSURANCE OF FOODS, J.E. Stauffer
THE SCIENCE OF MEAT AND MEAT PRODUCTS, 3RD ED., J.F. Price and
    B.S. Schweigert
HANDBOOK OF FOOD COLORANT PATENTS, F.J. Francis
ROLE OF CHEMISTRY IN THE QUALITY OF PROCESSED FOODS,
    O.R. Fennema, W.H. Chang and C.Y. Lii
NEW DIRECTIONS FOR PRODUCT TESTING AND SENSORY ANALYSIS
    OF FOODS, H.R. Moskowitz
PRODUCT TESTING AND SENSORY EVALUATION OF FOODS,
    H.R. Moskowitz
ENVIRONMENTAL ASPECTS OF CANCER: ROLE OF MACRO AND MICRO
    COMPONENTS OF FOODS, E.L. Wynder *et al.*
FOOD PRODUCT DEVELOPMENT IN IMPLEMENTING DIETARY
    GUIDELINES, G.E. Livingston, R.J. Moshy, and C.M. Chang
SHELF-LIFE DATING OF FOODS, T.P. Labuza
RECENT ADVANCES IN OBESITY RESEARCH, VOL. V, E. Berry,
    S.H. Blondheim, H.E. Eliahou and E. Shafrir
RECENT ADVANCES IN OBESITY RESEARCH, VOL. IV, J. Hirsch *et al.*
RECENT ADVANCES IN OBESITY RESEARCH, VOL. III, P. Bjorntorp *et al.*
RECENT ADVANCES IN OBESITY RESEARCH, VOL. II, G.A. Bray
RECENT ADVANCES IN OBESITY RESEARCH, VOL. I, A.N. Howard
ANTINUTRIENTS AND NATURAL TOXICANTS IN FOOD, R.L. Ory
UTILIZATION OF PROTEIN RESOURCES, D.W. Stanley *et al.*
FOOD INDUSTRY ENERGY ALTERNATIVES, R.P. Ouellette *et al.*
VITAMIN B_6: METABOLISM AND ROLE IN GROWTH, G.P. Tryfiates
HUMAN NUTRITION, 3RD ED., F.R. Mottram
FOOD POISONING AND FOOD HYGIENE, 4TH ED., B.C. Hobbs *et al.*
POSTHARVEST BIOLOGY AND BIOTECHNOLOGY, H.O. Hultin and M. Milner

Newsletters

FOOD INDUSTRY REPORT, G.C. Melson
FOOD, NUTRITION AND HEALTH, P.A. Lachance and M.C. Fisher
FOOD PACKAGING AND LABELING, S. Sacharow

STATEMENT OF OWNERSHIP, MANAGEMENT AND CIRCULATION
Required by 39 U.S.C. 3685)

1A. TITLE OF PUBLICATION	1B. PUBLICATION NO.	2. DATE OF FILING
Journal of Food Process Engineering	0 1 4 5 8 8 7 6	Oct. 1, 1987

3. FREQUENCY OF ISSUE	3A. NO. OF ISSUES PUBLISHED ANNUALLY	3B. ANNUAL SUBSCRIPTION PRICE
Quarterly	4	$80.00

4. COMPLETE MAILING ADDRESS OF KNOWN OFFICE OF PUBLICATION *(Street, City, County, State and ZIP+4 Code) (Not printers)*

FOOD & NUTRITION PRESS, INC.
6527 MAIN STREET, POB 583, TRUMBULL, FAIRFIELD, CONNECTICUT 06611

5. COMPLETE MAILING ADDRESS OF THE HEADQUARTERS OF GENERAL BUSINESS OFFICES OF THE PUBLISHER *(Not printer)*
FOOD & NUTRITION PRESS, INC., 6527 MAIN STREET, POB 583, TRUMBULL, CONNECTICUT 06611

6. FULL NAMES AND COMPLETE MAILING ADDRESS OF PUBLISHER, EDITOR, AND MANAGING EDITOR *(This item MUST NOT be blank)*

PUBLISHER *(Name and Complete Mailing Address)*
John J. O'Neil, 6527 Main Street, POB 583, Trumbull, Connecticut 06611

EDITOR *(Name and Complete Mailing Address)*

Dr. Dennis R. Heldman, National Food Processors Association, 1401 New York Ave.,NW
Washington, D.C. 20005
MANAGING EDITOR *(Name and Complete Mailing Address)*

Dr. R. Paul Singh, University of Calif., Dept. of Agricultural Engineering, Davis, CA 95616

7. OWNER *(If owned by a corporation, its name and address must be stated and also immediately thereunder the names and addresses of stockholders owning or holding 1 percent or more of total amount of stock. If not owned by a corporation, the names and addresses of the individual owners must be given. If owned by a partnership or other unincorporated firm, its name and address, as well as that of each individual must be given. If the publication is published by a nonprofit organization, its name and address must be stated.) (Item must be completed.)*

FULL NAME	COMPLETE MAILING ADDRESS
Food & Nutrition Press, Inc.	6527 Main Street, POB 583, Trumbull, CT 06611
John J. O'Neil	53 Stonehouse Rd.,Trumbull, CT 06611
Michael J. Tully	3 North Slope,Union Gap Village, Clinton, NJ
Kathryn O & Christopher R. Ziko	8 Maria Alicia Dr., Huntington, CT 06484
John J. O'Neil, Jr.	115 Maureen St., Stratford, CT 06497

8. KNOWN BONDHOLDERS, MORTGAGEES, AND OTHER SECURITY HOLDERS OWNING OR HOLDING 1 PERCENT OR MORE OF TOTAL AMOUNT OF BONDS, MORTGAGES OR OTHER SECURITIES *(If there are none, so state)*

FULL NAME	COMPLETE MAILING ADDRESS
None	

9. FOR COMPLETION BY NONPROFIT ORGANIZATIONS AUTHORIZED TO MAIL AT SPECIAL RATES *(Section 423.12 DMM only)*
The purpose, function, and nonprofit status of this organization and the exempt status for Federal income tax purposes *(Check one)*

(1) ☐ HAS NOT CHANGED DURING PRECEDING 12 MONTHS   (2) ☐ HAS CHANGED DURING PRECEDING 12 MONTHS   *(If changed, publisher must submit explanation of change with this statement.)*

10. EXTENT AND NATURE OF CIRCULATION *(See instructions on reverse side)*	AVERAGE NO. COPIES EACH ISSUE DURING PRECEDING 12 MONTHS	ACTUAL NO. COPIES OF SINGLE ISSUE PUBLISHED NEAREST TO FILING DATE
A. TOTAL NO. COPIES *(Net Press Run)*	450	450
B. PAID AND/OR REQUESTED CIRCULATION 1. Sales through dealers and carriers, street vendors and counter sales	0	0
2. Mail Subscription *(Paid and/or requested)*	310	303
C. TOTAL PAID AND/OR REQUESTED CIRCULATION *(Sum of 10B1 and 10B2)*	310	303
D. FREE DISTRIBUTION BY MAIL, CARRIER OR OTHER MEANS SAMPLES, COMPLIMENTARY, AND OTHER FREE COPIES	44	39
E. TOTAL DISTRIBUTION *(Sum of C and D)*	354	342
F. COPIES NOT DISTRIBUTED 1. Office use, left over, unaccounted, spoiled after printing	96	108
2. Return from News Agents	0	0
G. TOTAL *(Sum of E, F1 and 2—should equal net press run shown in A)*	450	450

11. I certify that the statements made by me above are correct and complete

SIGNATURE AND TITLE OF EDITOR, PUBLISHER, BUSINESS MANAGER, OR OWNER

John J. O'Neil, President

PS Form **3526,** Dec. 1985   *(See instruction on reverse)*
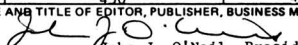
GUIDE FOR AUTHORS

Typewritten manuscripts in triplicate should be submitted to the editorial office. The typing should be double-spaced throughout with one-inch margins on all sides.

Page one should contain: the title, which should be concise and informative; the complete name(s) of the author(s); affiliation of the author(s); a running title of 40 characters or less; and the name and mail address to whom correspondence should be sent.

Page two should contain an abstract of not more than 150 words. This abstract should be intelligible by itself.

The main text should begin on page three and will ordinarily have the following arrangement:

Introduction: This should be brief and state the reason for the work in relation to the field. It should indicate what new contribution is made by the work described.

Materials and Methods: Enough information should be provided to allow other investigators to repeat the work. Avoid repeating the details of procedures which have already been published elsewhere.

Results: The results should be presented as concisely as possible. Do not use tables *and* figures for presentation of the same data.

Discussion: The discussion section should be used for the interpretation of results. The results should not be repeated.

In some cases it might be desirable to combine results and discussion sections.

References: References should be given in the text by the surname of the authors and the year. *Et al.* should be used in the text when there are more than two authors. All authors should be given in the Reference section. In the Reference section the references should be listed alphabetically. See below for style to be used.

DEWALD, B., DULANEY, J.T., and TOUSTER, O. 1974. Solubilization and polyacrylamide gel electrophoresis of membrane enzymes with detergents. In *Methods in Enzymology,* Vol. xxxii, (S. Fleischer and L. Packer, eds.) pp. 82–91, Academic Press, New York.

HASSON, E.P. and LATIES, G.G. 1976. Separation and characterization of potato lipid acylhydrolases. Plant Physiol. *57,*142–147.

ZABORSKY, O. 1973. *Immobilized Enzymes,* pp. 28–46, CRC Press, Cleveland, Ohio.

Journal abbreviations should follow those used in *Chemical Abstracts.* Responsibility for the accuracy of citations rests entirely with the author(s). References to papers in press should indicate the name of the journal and should only be used for papers that have been accepted for publication. Submitted papers should be referred to by such terms as "unpublished observations" or "private communication." However, these last should be used only when absolutely necessary.

Tables should be numbered consecutively with Arabic numerals. The title of the table should appear as below:

Table 1. Activity of potato acyl-hydrolases on neutral lipids, galactolipids, and phospholipids

Description of experimental work or explanation of symbols should go below the table proper. Type tables neatly and correctly as tables are considered art and are not typeset. Single-space tables.

Figures should be listed in order in the text using Arabic numbers. Figure legends should be typed on a separate page. Figures and tables should be intelligible without reference to the text. Authors should indicate where the tables and figures should be placed in the text. Photographs must be supplied as glossy black and white prints. Line diagrams should be drawn with black waterproof ink on white paper or board. The lettering should be of such a size that it is easily legible after reduction. Each diagram and photograph should be clearly labeled on the reverse side with the name(s) of author(s), and title of paper. When not obvious, each photograph and diagram should be labeled on the back to show the top of the photograph or diagram.

Acknowledgments: Acknowledgments should be listed on a separate page.

Short notes will be published where the information is deemed sufficiently important to warrant rapid publication. The format for short papers may be similar to that for regular papers but more concisely written. Short notes may be of a less general nature and written principally for specialists in the particular area with which the manuscript is dealing. Manuscripts which do not meet the requirement of importance and necessity for rapid publication will, after notification of the author(s), be treated as regular papers. Regular papers may be very short.

Standard nomenclature as used in the engineering literature should be followed. Avoid laboratory jargon. If abbreviations or trade names are used, define the material or compound the first time that it is mentioned.

CONTENTS